LMU LUDWIG-MAXIMILIANS-UNIVERSITÄT MÜNCHEN
CENTER FOR QUANTITATIVE RISK ANALYSIS
CEQURA

Holger Fink and Stefan Mittnik

Quanto pricing models beyond Black-Scholes

Working Paper Number 16, 2016
Center for Quantitative Risk Analysis (CEQURA)
Department of Statistics
University of Munich

http://www.cequra.uni-muenchen.de

QUANTO PRICING MODELS BEYOND BLACK-SCHOLES

HOLGER FINK[a,1], STEFAN MITTNIK[a,2]

ABSTRACT

The popularity of quanto options has constantly risen since their first introduction and new pricing models driven by normal tempered stable processes, have recently been introduced. However, as it is not easy to find a rich history of exchange recorded prices, empirical verification past plain vanilla options has been difficult. To overcome this obstacle, we resort to exchange-traded structured products: After deriving prices for composite options in the existing model framework we propose a new calibration procedure to overcome identification issues and carry out an extensive analysis of parameter stability as well as calibration performance for plain vanilla and exotic double barrier options.

AUTHORS INFO

[a]Chair of Financial Econometrics, Department of Statistics, Ludwig-Maximilians-Universität München, Akademiestrasse 1/I, 80799 Munich, Germany, Tel.: +49-89-21803224
[1]holger.fink@stat.uni-muenchen.de
[2]finmetrics@stat.uni-muenchen.de

KEYWORDS

normal tempered stable process, Lévy process, quanto options, Nikkei 225, calibration, parameter stability

JEL SUBJECT CLASSIFICATION

C58, G13, C52, C53, G17, G15

1. Introduction

Recent events in Japan starting with the 2012 general election that made Shinzo Abe prime minister brought the land of deflation and economic stagnation back into the focus of global investors. The main targets of the Abe administration were (and still are) bringing up inflation to 2%, weakening the Japanese yen and pushing for more growth. Therefore, it is only natural to ask how foreign investors can get exposure to the Japanese equity market represented, for example, by its lead index the Nikkei 225. Classical choices would either be a "direct" investment into this index or more risky leveraged strategies through options. However, both approaches may suffer from "Abenomics", the policy changes pushed by Japan's administration: Although an investor may benefit from rising equity prices, a weakening yen may wipe out any profit. A possible solution to tackle this problem is to resort to quanto options, i.e. derivatives where the exchange rate at maturity is fixed upfront.

To account for such features in classical option pricing models, one needs to model not only one but two tradable assets: the equity price and the foreign exchange (FX) rate – including the dependence structure between the two. Although such quanto derivatives have become increasingly popular over the years, academic literature on pricing models is scarce, with the standard setting being a two-dimensional Black-Scholes-type market, cf. Derman et al. (1990), Baxter and Rennie (1996) or Wilmott (2006). Recent publications include stochastic volatility extensions (Dimitroff et al. (2009)), Branger and Muck (2012) and Park et al. (2013)) or dynamic correlation models (Teng et al. (2015)). However, all these models are based on a multivariate Brownian motion, which is known not to capture the empirically observed heavy tails and asymmetric dependence in asset returns. Kim et al. (2015) were the first to leave this framework by specifying normal tempered stable (NTS) processes to drive asset dynamics. These represent a subtype of the rich Lévy class, which has been in the focus of market modeling since the early work of Eberlein and Keller (1995) and Eberlein et al. (1998). In particular, NTS processes were constructed in Barndorff-Nielsen and Levendorskii (2001) by time-changed Brownian motions and have been investigated since then especially in the context of portfolio analysis and option pricing, cf. Barndorff-Nielsen and Shephard (2001), Kim et al. (2012) or Fink et al. (2016). Very recently, Ballotta et al. (2015) formulated a general multivariate Lévy framework for combined

equity and FX markets to investigate model-implied correlations based on USD-denominated CME Nikkei 225 futures and plain vanilla options.

Kim et al. (2015) introduced the NTS model to price quanto options but, except from a short application using synthetic prices for illustration purposes, did not provide an empirical investigation. As they pointed out, exchange traded quanto options – especially beyond plain vanilla contracts – are hard to obtain and price histories of OTC trades are – per definition – not available.

In the current paper, we fill this gap and conduct a thorough empirical examination of the NTS quanto model. In order to achieve this, we consider two types of exchange-traded warrants which are a special class of retail structured products (RSPs): plain vanilla and exotic double-barrier options. For these kind of derivatives, as detailed in Section 3, market makers provide not only constant liquidity but also enable us to use exchange-recorded daily closing prices to compare different quanto pricing models beyond vanilla calls and puts. As conjectured in Kim et al. (2015), our analysis shows that the NTS model clearly outperforms the Gaussian model framework.

The paper is structured as follows. Section 2 presents the classical Black-Scholes-type setup and the newly introduced NTS framework of Kim et al. (2015), stating model assumptions and pricing formulas. Furthermore, estimation results using historical return data are presented while additional parameter restrictions for the NTS setup are motivated. Our data set of RSP prices is described in detail in Section 3. Section 4 then takes a first look by "naively" calibrating the known pricing formula to real market prices. Although the results look very much in favor of the NTS assumption, we will show that parameter identification and stability can be an issue. In Section 5, to overcome these obstacles, we theoretically extend the NTS model and provide certain pricing formulas for composite (compo) options on the stock and the FX rate individually. By using these price representations and combining historical estimation with risk-neutral calibration, we tackle the mentioned stability and identification issues while leaving the main advantages of the NTS model untouched. A brief summary closes the paper.

2. The NTS framework for quanto options

Following the theoretical setup of Kim et al. (2015) we model quanto options under two different assumptions: a two-dimensional NTS framework, the object of interest, and, for reference purposes, the classical Black-Scholes-type market. For both setups, we assume the existence of two riskless rates: Let $r_d \geq 0$ and $r_f \geq 0$ be the instantaneous interest rates for the domestic and foreign currency alike. In particular, there is one riskless (domestic) bank account denoted by

$$B = \{B(t)\}_{t\geq 0} \quad \text{with} \quad B(t) = \exp\{r_d t\}, \quad t \geq 0.$$

In our empirical study below, the domestic currency shall be the euro (EUR) and the foreign currency the Japanese yen (JPY)[1]. Furthermore we assume the existence of two tradable risky assets:

$$V = \{V(t)\}_{t\geq 0}$$

denotes the price process of an equity-type asset in the domestic currency (the Nikkei 225 index converted into EUR), while

$$\exp\{r_f \cdot\} F = \{\exp\{r_f t\} F(t)\}_{t\geq 0}$$

describes the (tradable) exchange rate process from the domestic (EUR) to the foreign currency (JPY); i.e., at time $t \geq 0$, an investor gets for one unit of foreign currency (JPY) $F(t)$ units of the domestic numéraire (EUR). We want to stress the importance of the factor "$\exp\{r_f t\}$": Any investment in the foreign currency would incur an interest rate payment of r_f. So, while F itself shall be the FX spot rate, it can only be traded via the foreign cash bond $\exp\{r_f \cdot\} F$. By combining both, we obtain the equity asset's price process in the foreign currency (the Nikkei 225 index in JPY),

[1] To avoid any confusion, we will from now on also always state the proper asset or currency in question in parentheses.

given by

$$N = \{N(t)\}_{t\geq 0} = \left\{\frac{V(t)}{F(t)}\right\}_{t\geq 0}.$$

2.1 Remark (Model summary). *(i) Below, EUR will be our domestic currency as we consider quanto options traded on the Frankfurt Exchange in EUR. N then denotes the Nikkei 225 in the "foreign" currency JPY (from a European investors perspective) although strictly speaking JPY is the "real" domestic currency for the Nikkei 225.*
(ii) Even though there are two riskless interests rates in our model, r_d and r_f, there is only one riskless bank account B which is denoted in the domestic currency. A similar object, accruing with r_f, would be subject to exchange rate risk and is given by $\exp\{r_f\cdot\}F$.

Given this general market framework, we first specify the (simpler) Black-Scholes-type setting making the following assumptions:

2.2 Assumption (Black-Scholes setting, cf. Kim et al. (2015), Section 3.1). *Let $W = (W_X,\bar{W}_Y) = \{(W_X(t),\bar{W}_Y(t))\}_{t\geq 0}$ be a two-dimensional standard Brownian motion with independent marginal processes. Furthermore, let $\mu_X,\mu_Y \in \mathbb{R}$, $\sigma_X,\sigma_Y > 0$ and $\rho \in [-1,1]$. To construct a suitable but straightforwardly traceable dependence between the equity asset, V, and the FX rate, F, we set*

$$W_Y := \rho W_X + \sqrt{1-\rho^2}\bar{W}_Y$$

which leads to $\mathbb{C}\mathrm{orr}(W_X(t),W_Y(t)) = \rho t$ for $t \geq 0$. With $V(0) > 0$ and $F(0) > 0$ assume the following dynamics under the real-world measure $\mathbb{P}$ for $t \geq 0$

$$V(t) = V(0)\exp\{\mu_X t + \sigma_X W_X(t)\}, \quad F(t) = F(0)\exp\{\mu_Y t + \sigma_Y W_Y(t)\}.$$

To price quanto options, the above setup needs to be arbitrage-free with the usually considered class of admissible trading strategies (cf. Delbaen and Schachermayer (1994)) and construct a suitable equivalent martingale measure. Since we have two tradable assets and two sources of risk, both given by Brownian motions, we have the following theorem.

2.3 Theorem (cf. Kim et al. (2015), Section 3.1). *In the situation of Assumption 2.2 let $\rho^2 \neq 1$. Then, there exists a unique equivalent measure $\mathbb{Q}$ under which*

$$\begin{aligned} V(t) &= V(0)\exp\{r_d t - \frac{\sigma_X^2}{2}t + \sigma_X B_X(t)\}, \\ F(t) &= F(0)\exp\{(r_d - r_f)t - \frac{\sigma_Y^2}{2}t + \sigma_Y\rho B_X(t) + \sigma_Y\sqrt{1-\rho^2}\bar{B}_Y(t)\} \end{aligned}$$

for $t \geq 0$. and where $B = (B_X,\bar{B}_Y) = \{(B_X(t),\bar{B}_Y(t))\}_{t\geq 0}$ is a two-dimensional standard Brownian motion with independent marginal processes. Furthermore, the discounted tradable assets $\{\exp\{-r_d t\}V(t)\}_{t\geq 0}$ and $\{\exp\{-(r_d - r_f)t\}F(t)\}_{t\geq 0}$ are $\mathbb{Q}$-martingales.

Let $T > 0$, then the price, $C_t(K,T)$, of a European quanto call option on $N(T)$ with strike $K > 0$ at time $0 \leq t \leq T$ is given by

$$\begin{aligned} C_t^{quanto}(K,T) &= \exp\{-r_d(T-t)\}\mathbb{E}^{\mathbb{Q}}[F_{fix}(N(T)-K)^+|\mathcal{F}_t] \\ &= F_{fix}\Big(e^{(r_f - r_d + \sigma_Y^2 - \rho\sigma_X\sigma_Y)(T-t)}N(t)\Phi(d_1) - e^{-r_d(T-t)}K\Phi(d_2)\Big) \end{aligned} \tag{1}$$

where

$$\begin{aligned} d_1 &= \frac{\log(N(t)/K) + (r_f + \sigma_Y^2 - \rho\sigma_X\sigma_Y + \frac{1}{2}[\sigma_X^2 - 2\sigma_X\sigma_Y\rho + \sigma_Y^2])(T-t)}{\sqrt{[\sigma_X^2 - 2\sigma_X\sigma_Y\rho + \sigma_Y^2]}\sqrt{T-t}}, \\ d_2 &= d_1 - \sqrt{[\sigma_X^2 - 2\sigma_X\sigma_Y\rho + \sigma_Y^2]}\sqrt{T-t}. \end{aligned}$$

Here $(\mathcal{F}_t)_{\geq 0}$ is the (augmented) filtration generated by V and F which we can assume to satisfy the usual conditions of right-continuity and completeness.

Having set up our reference model, we now turn to the NTS setting of Kim et al. (2015), the object of interest in our empirical study.

2.4 Assumption (NTS market setting, cf. Kim et al. (2015), Section 3.2)**.** *Let $\mathcal{T} = \{\mathcal{T}(t)\}_{t\geq 0}$ be a tempered stable subordinator, i.e., an a.s. increasing Lévy process with characteristic function*

$$\mathbb{E}\Big[\exp\{iu\mathcal{T}(t)\}\Big] = \exp\Big\{-\frac{2t\theta^{1-\frac{\alpha}{2}}}{\alpha}\Big[(\theta - iu)^{\frac{\alpha}{2}} - \theta^{\frac{\alpha}{2}}\Big]\Big\}, \quad u \in \mathbb{R}, \quad t \geq 0,$$

with $\alpha \in (0,2]$ and $\theta > 0$. For a two-dimensional standard Brownian motion $B = (B_X, B_Y) = \{(B_X(t), B_Y(t))\}_{t\geq 0}$ with correlated marginal processes, independent of $\mathcal{T}$, construct a two-dimensional NTS process $(X,Y) = \{(X(t), Y(t))\}_{t\geq 0}$ by

$$\begin{pmatrix} X(t) \\ Y(t) \end{pmatrix} = \begin{pmatrix} \mu_X \\ \mu_Y \end{pmatrix} t + \begin{pmatrix} \beta_X \\ \beta_Y \end{pmatrix} [\mathcal{T}(t) - t] + \begin{pmatrix} \sigma_X & 0 \\ 0 & \sigma_Y \end{pmatrix} \begin{pmatrix} B_X(\mathcal{T}(t)) \\ B_Y(\mathcal{T}(t)) \end{pmatrix} \tag{2}$$

with $\mu_X, \mu_Y, \beta_X, \beta_Y \in \mathbb{R}$, $\sigma_X, \sigma_Y > 0$ and $\mathbb{C}\mathrm{orr}(B_X(t), B_Y(t)) = \rho t$, $t \geq 0$, $\rho \in [-1,1]$. We write

$$(X,Y) \sim \mathrm{NTS}_2\left(\alpha, \theta, \begin{bmatrix} \mu_X \\ \mu_Y \end{bmatrix}, \begin{bmatrix} \beta_X \\ \beta_Y \end{bmatrix}, \begin{bmatrix} \sigma_X \\ \sigma_Y \end{bmatrix}, \begin{bmatrix} 1 & \rho \\ \rho & 1 \end{bmatrix}\right).$$

Furthermore, with $V(0) > 0$ and $F(0) > 0$, we assume the following dynamics for our tradable assets under the real-world measure $\mathbb{P}$ for $t \geq 0$:

$$V(t) = V(0)\exp\{X(t)\}, \quad F(t) = F(0)\exp\{Y(t)\}.$$

It is well known that subordinated (i.e., time-changed) Lévy processes are again of the Lévy type. Therefore, all measure changes under which the Lévy property is invariant basically modify the deterministic drift and the jump intensity[2]. Choosing such a measure change (in particular one of the Escher transform type) and defining the functions

$$\begin{aligned} w_X : \Big(-\infty, \theta - \beta_X - \frac{\sigma_X^2}{2}\Big) &\to \infty \\ \lambda_X^\star &\mapsto -\beta_X - \frac{2\theta^{1-\frac{\alpha}{2}}}{\alpha}\Big[\Big(\theta - \beta_X - \lambda_X^\star - \frac{\sigma_X^2}{2}\Big)^{\frac{\alpha}{2}} - \theta^{\frac{\alpha}{2}}\Big] \end{aligned}$$

and

$$\begin{aligned} w_Y : \Big(-\infty, \theta - \beta_Y - \frac{\sigma_Y^2}{2}\Big) &\to \infty \\ \lambda_Y^\star &\mapsto -\beta_Y - \frac{2\theta^{1-\frac{\alpha}{2}}}{\alpha}\Big[\Big(\theta - \beta_Y - \lambda_Y^\star - \frac{\sigma_Y^2}{2}\Big)^{\frac{\alpha}{2}} - \theta^{\frac{\alpha}{2}}\Big], \end{aligned}$$

[2] cf. Theorems 33.1 and 33.2 of Sato (1999)

Kim et al. (2015) proved the following theorem.

2.5 Theorem (Kim et al. (2015), Section 3.2 and Theorem 3.1)**.** *Let Assumption 2.4 hold with* $\rho^2 \neq 1$ *and suppose that there are*

$$\lambda_X^\star < \theta - \beta_Y - \frac{\sigma_Y^2}{2} \quad \text{and} \quad \lambda_Y^\star < \theta - \beta_Y - \frac{\sigma_Y^2}{2}$$

such that

$$\mu_X - r_d + w_X(\lambda_X^\star) = 0 \quad \text{and} \quad \mu_Y - r_d + r_f + w_Y(\lambda_Y^\star) = 0.$$

Then, there exists an equivalent measure $\mathbb{Q}$ *under which*

$$V(t) = V(0)\exp\{(r_d - w_X(\lambda_X^\star))t + X(t)\}, \quad F(t) = F(0)\exp\{(r_d - r_f - w_Y(\lambda_Y^\star))t + Y(t)\},$$

for $t \geq 0$*, with*

$$(X,Y) \sim \mathrm{NTS}_2\left(\alpha,\theta,\begin{bmatrix}\lambda_X^\star\\ \lambda_Y^\star\end{bmatrix},\begin{bmatrix}\beta_X+\lambda_X^\star\\ \beta_Y+\lambda_Y^\star\end{bmatrix},\begin{bmatrix}\sigma_X\\ \sigma_Y\end{bmatrix},\begin{bmatrix}1 & \rho\\ \rho & 1\end{bmatrix}\right).$$

The discounted tradable assets $\{\exp\{-r_d t\}V(t)\}_{t\geq 0}$ *and* $\{\exp\{-(r_d - r_f)t\}F(t)\}_{t\geq 0}$ *are* $\mathbb{Q}$*-martingales.*

Let $T > 0$*, then the price,* $\mathcal{C}_t(K,T)$*, of a European quanto call option on* $N(T)$ *with strike* $K > 0$ *at time* $0 \leq t \leq T$ *is given by*

$$\begin{aligned}\mathcal{C}_t^{quanto}(K,T) &= \exp\{-r_d(T-t)\}\mathbb{E}^{\mathbb{Q}}[F_{fix}(N(T)-K)^+|\mathcal{F}_t]\\ &= \frac{e^{-r_d(T-t)}F_{fix}K^{1+\zeta}}{2\pi N(t)^\zeta e^{\zeta(r_f - w_X(\lambda_X^\star)+w_Y(\lambda_Y^\star))(T-t)}}F\Big(\frac{1}{2\pi}\log\Big(\frac{K}{N(t)}\Big)\Big),\end{aligned} \tag{3}$$

where

$$F(x) = \int_{\mathbb{R}} e^{-2\pi i u x}\frac{e^{iu(r_f - w_X(\lambda_X^\star)+w_Y(\lambda_Y^\star))(T-t)}}{(iu-\zeta-1)(iu-\zeta)}\mathbb{E}\Big[e^{(iu-\zeta)Z(T-t)}\Big]du$$

with $Z = X - Y$ *and* $\zeta \in \mathbb{R}$ *such that the appearing moment generating function exists. Again,* $(\mathcal{F}_t)_{\geq 0}$ *is the augmented filtration generated by* V *and* F *and satisfying the usual conditions of right-continuity and completeness.*

As pointed out in Kim et al. (2015), the call price formula (which is derived by classical Fourier pricing methods, cf. Carr and Madan (1999)) can be efficiently evaluated by the Fast Fourier Transform algorithm.

We close this section by presenting parameter estimates using daily return data as shown in Figure 1. The data covers 04 January 2000 to 15 April 2013[3]. The annualized parameter estimates, by maximum likelihood based on inversion of the characteristic functions of the NTS setup, are reported in Table 1[4]. Given the confidence interval of the tail parameter α, the NTS model is historically clearly separated from the Gaussian setup. Furthermore, both market models produce a modest positive correlation. However, when interpreting this effect, we need to be aware that V describes the Nikkei 225 in EUR not in JPY. Given that, in the Gaussian case,

$$\mathbb{C}\mathrm{orr}\left(\log\frac{N(t)}{N(t-1)},\log\frac{F(t)}{F(t-1)}\right) = \frac{\sigma_X\sigma_Y\rho - \sigma_Y^2}{\sqrt{\sigma_X^2 - 2\sigma_X\sigma_Y\rho + \sigma_Y^2}\sigma_Y}. \tag{4}$$

Our parameter estimates imply a correlation of -0.4691 between the log returns of N and F, i.e., a strengthening JPY is negatively correlated with the Nikkei 225 (in JPY), a relationship we expect given the export-orientation of the

[3] Our option data set will start on 16 April 2013, cf. Section 3.

[4] For the maximization procedure we additionally restricted ourselves to $\alpha \geq 1$ and $\theta \in [20,200]$ – which we will explain below.

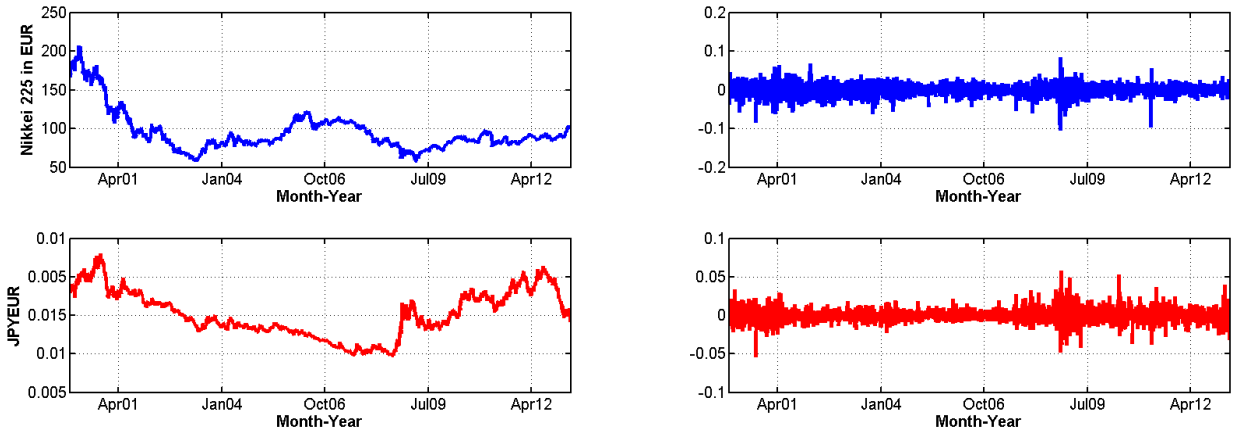

Figure 1: Top: Nikkei 225 in EUR (left) and its log returns (right). Bottom: JPYEUR levels (left) and log returns (right). All ranging from 04 January 2000 to 15 April 2013.

Japanese economy.

Figure 2 shows the estimated (log-)densities of both models for V, F and N. We want to stress an important observation, which has also been made by Kim et al. (2015) for the corresponding USD-based setup: The Black-Scholes model is not able to cope with the empirically observable fat tails, leading to a normal distribution which is more flat around its modus than the NTS model. We will come back to this drawback in Section 4 as it will have heavy implications when pricing double-barrier options.

It remains to explain why we imposed additional parameter restrictions to α and θ: Consider simulated paths of V/F with varying α and θ shown in Figure 3 (where the exact simulation procedure will be explained later in Section 4). As we can see, small tempering parameters θ imply very unrealistic sample paths with very large jumps. Furthermore, tail parameters α smaller than one lead to paths with finite variation (cf. Section 2 of Kim et al. (2015)). Additionally, if both are taken too small or if θ is very large, numerical instabilities can arise.

3. Data on retail structured products

Having set up the models to be investigated empirically, in this section, we discuss the data we will use for this purpose. As Kim et al. (2015) pointed out already, classical quanto options, like calls and puts, are rarely traded on official exchanges[5] and, per definition, OTC trades are not recorded by financial data providers and, thus, not available for empirical analyses.

However, the situation is better when turning to retail structured products (RSPs). Looking just at the German market (being one of the largest RSP markets in the world), several banks and issuers provide quanto structures to be tradable at retail exchanges. In this business, the issuer usually commits to continuously quote bid and offer prices which can be accessed.

Considering Nikkei 225 quanto RSPs, Société Générale appears to be the dominating player in this market niche in terms of available products[6]. For this reason and to avoid possible differences between issuers (cf. Remark 3.1 below), we focus on the French investment bank's products.

[5] CME options on its Nikkei 225 USD futures being one of the few exceptions.

[6] concentrating on simpler option types and leaving more complex structures like bonus-, lookback- or rainbow-certificates for future research

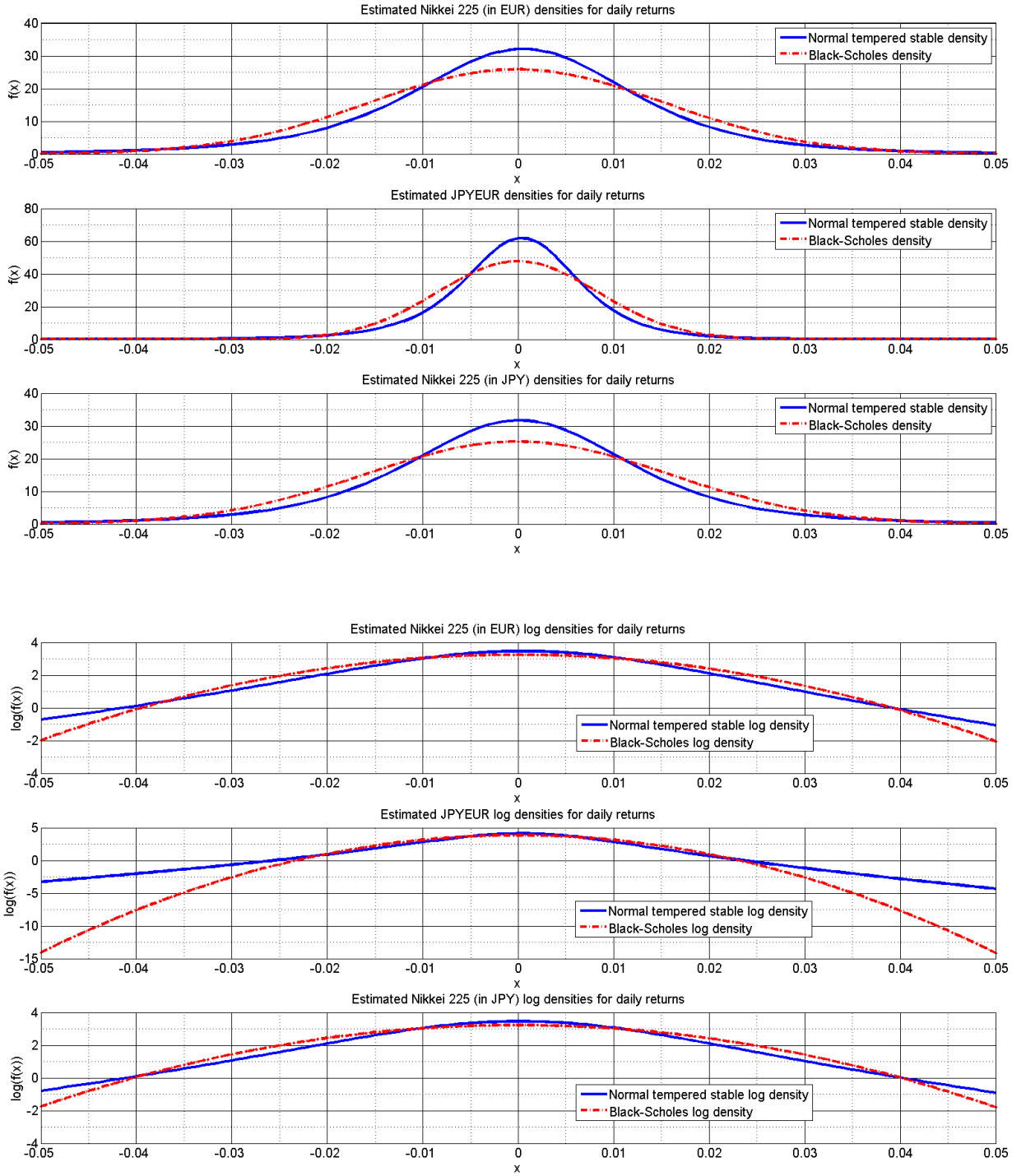

Figure 2: Estimated (log-)densities based on Table 1.

Parameters	Black-Scholes		NTS	
α	2	–	1.2962	[1.0662,1.4484]
θ	–	–	74.6539	[47.1372,127.7335]
μ_X	−0.0426	[−0.2401,0.1593]	−0.0454	[−0.1625,0.0732]
β_X	–	–	−0.3192	[−0.5694, – 0.0824]
σ_X	0.2434	[0.2341,0.2525]	0.2477	[0.2396,0.2559]
μ_Y	−0.0147	[−0.1180,0.0910]	−0.0165	[−0.0784,0.0450]
β_Y	–	–	0.2062	[0.0798,0.3403]
σ_Y	0.1319	[0.1270,0.1368]	0.1280	[0.1237,0.1321]
ρ	0.2216	[0.1724,0.2722]	0.2342	[0.1935,0.2770]

Nikkei 225 in EUR

log-likelihood	8.8344×10^3	8.9621×10^3
AIC	-1.7665×10^4	-1.7920×10^4
BIC	-1.7653×10^4	-1.7908×10^4

JPYEUR

log-likelihood	1.0800×10^3	1.1022×10^3
AIC	-2.1597×10^4	-2.2040×10^4
BIC	-2.1585×10^4	-2.2027×10^4

Table 1: Parameter estimates and bootstrapped 95% confidence intervals using 1,000 simulated paths of length 3,206 (inline with our historical return data set). For both time series, the likelihood ratio test can reject the Black-Scholes model on any reasonable significance level.

Our data set consists of 29 quanto call options on the Nikkei 225 (traded in EUR) and 363 digital knock-out (KO) options with upper and lower barriers also referred to as "inline options" or "double-barrier options", respectively. The later pay a fixed amount in EUR (10 EUR in our case) at maturity if the Nikkei 225 (in JPY) based on tick-by-tick observations has never touched or violated any of the barriers. Therefore, they can basically be classified as quanto KO options. In addition, we have 18 compo FX options (11 calls, 7 puts) on EURJPY and 20 compo calls on the Nikkei 225, both types with EUR as a base currency. All price series are shown in Figure 4.

Daily closing bid prices were obtained from the data provider "ARIVA.DE AG" which also supplies the Frankfurt retail exchange "Börse Frankfurt Zertifikate AG". The sample period we consider ranges from 16 April 2013 (issue date) to 15 September 2014 for the plain vanilla options and from 19 June 2013 to 15 September 2014 for the KO warrants, covering a total period of 17 months – a samples size that is inline with similar studies (e.g., Guillaume (2013)). After removing trading days where recordings are missing, we are left with a total of 354 daily observations.

Since the Japanese markets are closed at the time the option prices are recorded, we rely on the price of a quanto Nikkei 225 open-end-tracker issued and priced by Société Générale. This American product gives the buyer the right to exercise it with a three-month notice period every year on November 26 and to receive the Nikkei 225 close on this Japanese trading day (ratio 100:1). The spread of this product is quite tight and one can expect these kind of RSPs not to contain much margin for the issuer (cf. Remark 3.1). As direct consequence, its pricing should closely resemble Société Générale's proprietary Nikkei 225 indication. As for the EURJPY rate, we compare several issuers' quanto and compo Nikkei 225 tracker and implicitly derive the (mean) FX rate[7].

3.1 Remark. *As we are looking at RSPs (plain vanilla and double-barrier options) there are some potential sources of systemic bias from the 'fair model price' which we need to address.*

(i) ***Credit risk****: All products are basically a type of bearer bonds and, thus, are expected to include counterparty risk. Therefore, one would assume, considering only this effect, tradable prices to be somewhat lower than those*

[7]The identifiers ("WKNs") of these tracker and the above plain vanilla and KO options are provided in the appendix.

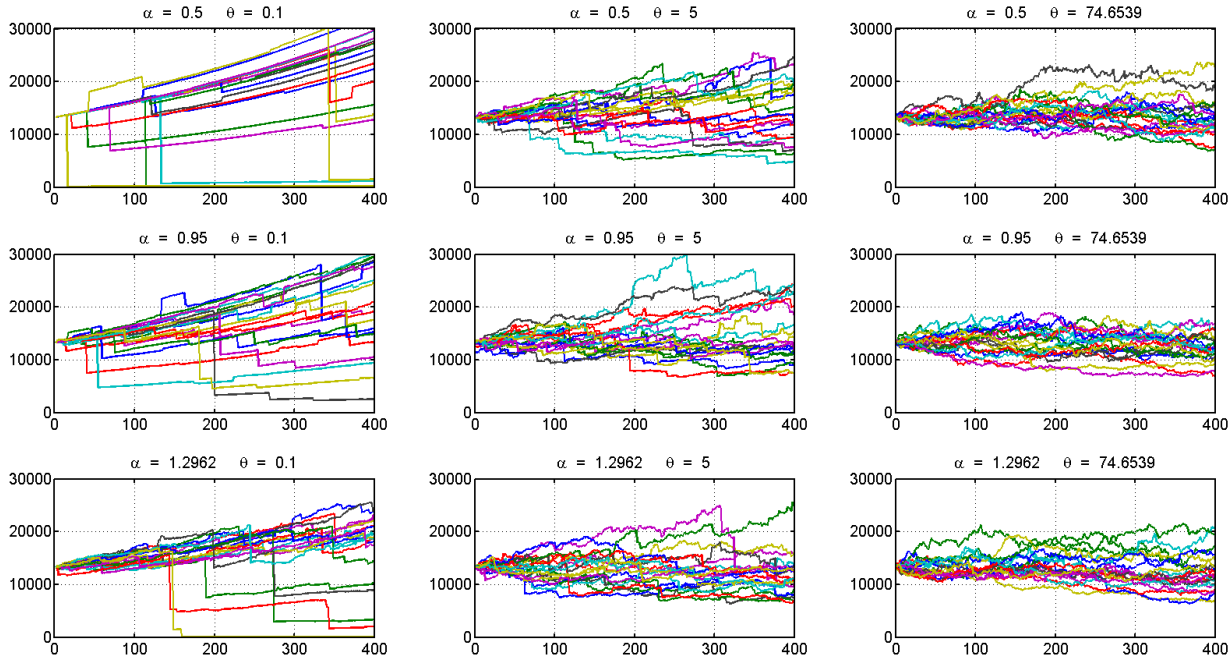

Figure 3: Simulated NTS paths of V/F for varying α and θ. Remaining parameters were held fixed (cf. Table 1).

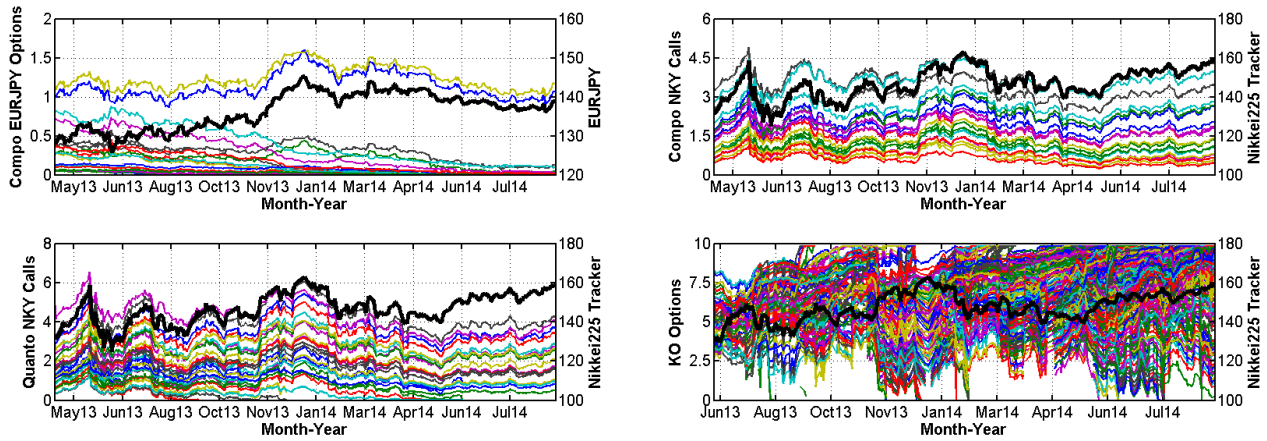

Figure 4: Top: Société Générale's compo EURJPY options calls (left) and compo Nikkei 225 calls together with Nikkei 225 tracker (right). Bottom left: Société Générale's quanto calls and Nikkei 225 tracker. Bottom right: Société Générale's KO options and Nikkei 225 tracker. Vanilla (compo & quanto) contracts ranging from 16 April 2013 to 15 September 2014. KO options ranging from 19 June 2013 to 15 September 2015.

coming from classical option pricing models as investors would want to be compensated for taking on default risk.

(ii) ***Issuer's PnL****: Issuers intend to profit from structuring and pricing RSPs which is reflected in the "overpricing-" and the "lifecycle-hypothesis". "Overpricing" means a certain margin is charged on top of the model price (cf. Chen and Kensinger (1990) and Chen and Sears (1990) for the US retail market and Wilkens et al. (2003) for Germany). According to the "lifecycle-hypothesis", this charge tends to decrease over time as the issuer presumably wants to profit from initial investors selling back later (cf. Stoimenov and Wilkens (2005)).*

(iii) ***Dividends****: The Nikkei 225 is a price index and, thus, does not account for dividends. Therefore, all else being equal, the index would decrease over time through this effect. The chosen market setups (Black-Scholes and NTS alike) do not account for such dividends.*

However, the bias may not be that dramatic as these three effects may offset each other to some extend: Sources (i) *and* (iii) *cause model prices to be higher than the real market prices, while not incorporating* (ii)*, would induce lower model-implied quotes.*

4. "Naive" model calibration using quanto options

As stated above, our goal is to empirically compare the NTS assumption with the classical Gaussian benchmark. The later is known to be deficient, especially when it comes to more exotic payoffs, as significant risks, like jump or tail risk, might be underpriced. Therefore, our study will be based on two types of comparison: the in-sample fit, by calibrating parameters to classical vanilla options, and the out-of-sample fit via pricing exotic double-barrier derivatives.

We first use the vanilla options to calibrate the parameters for each trading day, compare the models' fit to the data (in-sample-fit). Afterwards, we calculate *delta-based* forecasts to assess parameter stability, i.e., we plug yesterday's parameters into today's pricing formula. The main input factor (apart from time to maturity and interest rates) that changes is the price of the underlying, giving rise to the naming in the context of the Black-Scholes Greek "delta". We follow Teng et al. (2015) and minimize the relative mean square error (RelMSE) to calibrate the models, i.e., we chose the respective parameters collected in the vector $\Theta_t^\star$ by minimizing[8] the daily RelMSE between market and model prices or, formally,

$$\Theta_t^\star = \operatorname{argmin}_\Theta \mathrm{RelMSE}(\Theta)_t := \operatorname{argmin}_\Theta \left\{ \frac{1}{n_t} \sum_{i=1}^{n_t} \frac{\left[P_t^{\mathrm{model}}(K_i,T_i|\Theta) - P_t^{\mathrm{market}}(K_i,T_i) \right]^2}{P_t^{\mathrm{market}}(K_i,T_i)} \right\},$$

where n_t denotes the number of available prices on day t. As starting points for the Black-Scholes pricing we choose the historical volatilities and correlation of the Nikkei 225 in EUR and the EURJPY exchange rate obtained by maximum likelihood estimation (cf. Table 1). For the NTS calibration, we start with the implied Black-Scholes volatilities and correlation and set the other initial values additionally to $\alpha = 1.5$, $\theta = 25$ and $\mu_X = \mu_Y = \beta_X = \beta_Y = 0$. The semi-analytic formula (3) is approximated by the Fast Fourier Transform algorithm. To avoid any numerical instabilities for $\alpha \approx 2$, we restricted ourselves to $\alpha \in [1,1.95] \cup \{2\}$ and $\theta \in [20,200]$ (cf. the discussion at the end of Section 2).

For our second comparison, we use the obtained daily parameters to assess the one-day out-of-sample model fit by pricing the KO warrants described in Section 3. This, however, is not straightforward, since pricing such barrier options amounts to knowing the distribution of the running minimum and maximum of the underlying price process. For Black-Scholes-type settings, this problem has been considered by Kunitomo and Ikeda (1992) and by Geman and Yor (1996), and sensible formulas for implementation are available.

[8] The minimization is carried out in MATLAB using the routine "fmincon". For this procedure the pricing formulas from Section 2 are invoked.

For general Lévy markets (as the NTS setup) several solutions are possible[9], but there is no simple analytic formula. Besides classical simulation-based Monte Carlo methods, which we will make use here, other numerical or semi-analytical approaches include partial integro-differential equations (PIDEs) and Fourier methods[10]. As NTS processes are partially generated by time-changed Brownian motions, the work of Escobar et al. (2014) is also closely related to our setup, but differs in that our subordinator, appearing in the NTS definition, is a jump process.

All these studies focus on continuous barriers. In reality, a continuous observation is impossible. In fact, the considered KO options observe the barrier only when Nikkei 225 prints are available, which is every 15 seconds, five hours per trading day. Therefore, when using PIDE or Fourier methods, some kind of continuity correction would be necessary as well (see Broadie and Glasserman (1997) for the Gaussian case). To avoid this, we rely on simulation-based pricing which suffices for our objectives. The general idea is as follows: For a double-barrier option with maturity T, upper barrier K^u and lower barrier K^l we simulate M sample paths $\{\tilde{N}_i(t)\}_{0\le t\le T}$, $i \in \{1,\dots,N\}$, under $\mathbb{Q}$ and approximate for $t \le T$

$$\begin{aligned} & \mathcal{KO}_t(K^u,K^l,T) = \exp\{-r_d(T-t)\}\mathbb{E}^{\mathbb{Q}}[10\,\text{EUR} \times \mathbf{1}_{\{K^l<\min_{t\le T} N(t),\, \max_{t\le T} N(t)<K^u\}}|\mathcal{F}_t] \\ \approx\ & 10\,\text{EUR} \times \frac{\exp\{-r_d(T-t)\}}{M} \sum_{i=1}^{M} \mathbf{1}_{\{K^l<\min_{t\le T}\tilde{N}(t)\}} \mathbf{1}_{\{\max_{t\le T}\tilde{N}(t)<K^u\}} \end{aligned}$$

under the restriction, that none of the barriers have been touched until $t \ge 0$[11]. The main challenge (besides the computational burden) is now to simulate from the NTS distribution. In the light of (2) and an application of classical Euler-Maruyama schemes, this basically boils down to obtaining realizations from the driving tempered stable subordinator. Potential solutions include sampling by an infinite series representation, as applied, for example, by Bianchi et al. (2010) or numerically inverting the cumulative distribution function (which can itself be obtained by Fourier transformation of the characteristic function). However, since we need – to be inline with real Nikkei 225 prints – price paths simulated on a 15 second grid, these approaches are not sensible from a computational perspective for such a thin discretization.

A practical solution is provided by an acceptance-rejection scheme which performs best for such dense time grids (cf. Baeumer and Meerschaert (2010) and Kawai and Masuda (2012)). Following the notation of Algorithm 3 in Kawai and Masuda (2012), the simulation of $\mathcal{T}(\Delta t)$, $\Delta t \ge 0$, consists of the following steps:

Step 1: Generate independently $U \sim \text{Uniform}(0,1)$, $U' \sim \text{Uniform}(-\pi/2,\pi/2)$ and $E \sim \text{Exponential}(1)$.

Step 2: Calculate

$$V = \left(\Delta t \frac{-2\theta^{1-\frac{\alpha}{2}}}{\alpha\Gamma(-\frac{\alpha}{2})}\right)^{\frac{2}{\alpha}} \left(\frac{2\Gamma(1-\frac{\alpha}{2})}{\alpha\cos(U')}\right)^{\frac{2}{\alpha}} \sin\left(\frac{\alpha}{2}(U'+\pi/2)\right)\left(\frac{\cos\left(U'-\frac{\alpha}{2}(U'+\pi/2)\right)}{E}\right)^{\frac{2-\alpha}{\alpha}}$$

Step 3: If $U \le \exp\{-\theta V\}$, return V. Otherwise return to Step 1.

For $\Delta t \to 0$, the acceptance probability converges to 1 (cf. Baeumer and Meerschaert (2010) and Kawai and Masuda (2012)) and, therefore, this setup is perfectly suited for our purposes.

For all considerations, riskless rates were taken to be the lending rates from the European Central Bank and the Bank of Japan, respectively, at each trading day of the observation period.

[9] A very good overview and description of the various techniques can be found in Eberlein et al. (2009, 2010) or Eberlein and Glau (2014) and references therein.

[10] The latter one relying on the so called Wiener-Hopf factorization leading to approximations of the running minimum and maximum's characteristic functions and has been successfully applied for variance-gamma-type Lévy models (cf. Schoutens and Van Damme (2011))

[11] It should be mentioned that in case of a knock-out, these kind of products usually still pay a fixed amount of 0.001 EUR for tax purposes. For simplicity however, we shall ignore this feature.

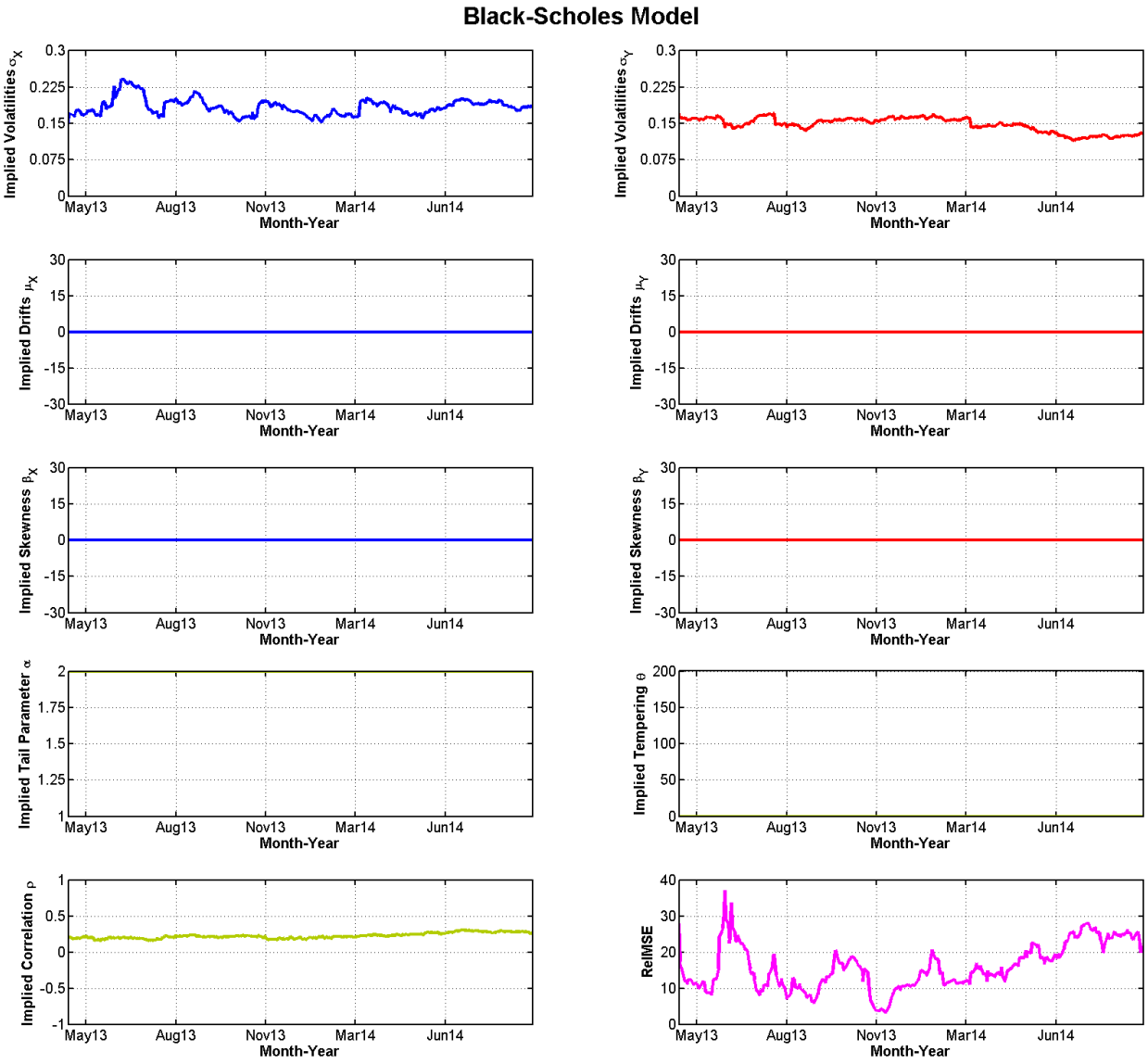

Figure 5: Quanto Calls: daily calibrated Black-Scholes parameters and RelMSE. All ranging from 16 April 2013 to 15 September 2014.

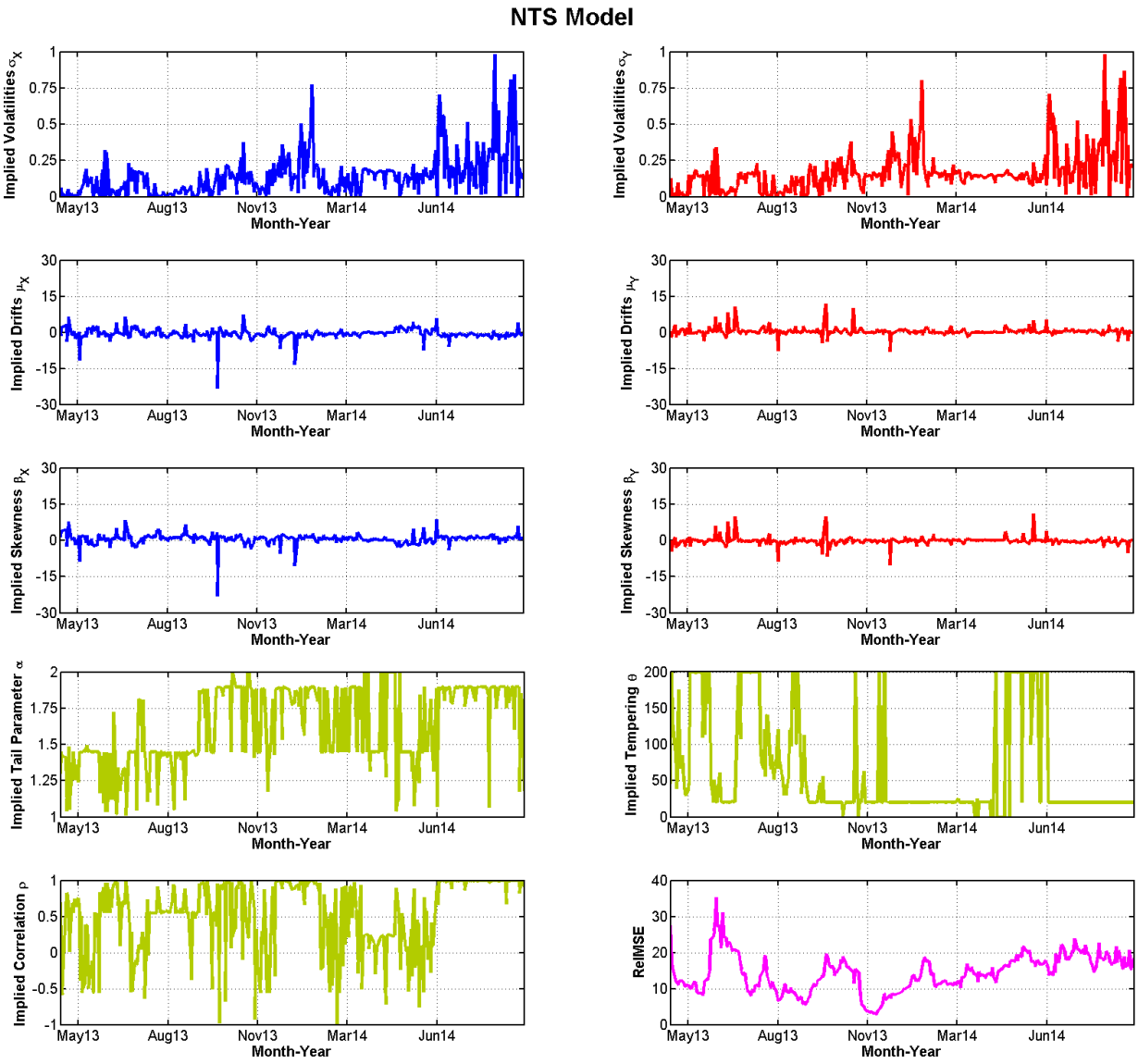

Figure 6: Quanto Calls: daily calibrated implied (X,Y) NTS parameters and RelMSE. All ranging from 16 April 2013 to 15 September 2014.

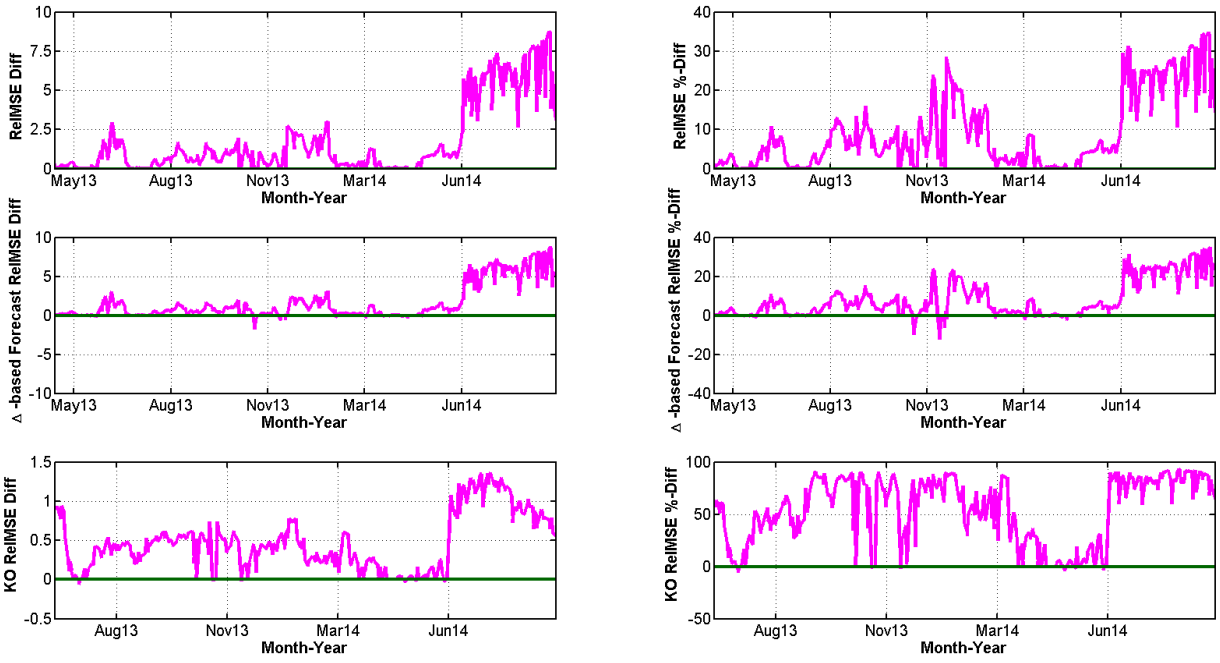

Figure 7: Quanto calls and KO options. Top: RelMSE-difference for the calibration. Middle: RelMSE-difference of the *delta-based* forecasts. Both ranging from 16 April 2013 to 15 September 2014. Bottom: RelMSE-difference using the respective calibrated parameters from 19 June 2013 to 15 September 2014. Calculations were based on 20,000 sample paths simulated on each considered trading day assuming 5 daily trading hours and sampling every 15 seconds. Positive values indicate better performance of the NTS model.

Let us turn to the empirical results: The daily implied parameters and RelMSE for the Black-Scholes model are plotted in Figure 5. To facilitate comparisons of the two models, the graphical summary also includes plots of the implied drift, skewness, tempering and tail calibration series which are set to 0 and 2, respectively. The results for the NTS calibration are presented in Figure 6. The following points are worth noting:

First, the Black-Scholes correlation seems always to be close to zero and the implied volatilities themselves are negatively correlated. In fact, various numerical tests show that the calibrated parameters are sensitive to the chosen starting values without affecting, however, the RelMSE itself. This indicates identification problems when just considering quanto options. We will discuss this in more detail in Section 5.

Second, the tail and tempering parameters α and θ in the NTS setting show a high variation and seem to be quite instable over time. This is especially visible for α and is inline with the results on artificial quanto prices of Kim et al. (2015). This fluctuation has a strong impact on the other calibrated parameters. For example, $\alpha = 2$ implies a Black-Scholes market, where $\mu_X, \mu_Y, \beta_X, \beta_Y$ and θ have no pricing consequence at all, while their influence becomes stronger for smaller α-values.

Finally, in Figure 7 we compare both models in terms of their daily RelMSE, the *delta-based* forecast and the double-barrier option pricing:

First, as the Black-Scholes model is contained in the NTS framework, RelMSE differences are non-negative and positive values support the NTS model. While on some days both models seem to fit equally well with respect to the data, the NTS setup generally outperforms.

Second, we find that even though parameter stability seems to be an issue for the NTS model as well, using yesterday's parameters leads still to more realistic model prices than in the Black-Scholes setup. This has a large impact for practical applications: When traders price derivatives, they always have to rely on available model parameters.

Third, when considering barrier risk, the NTS setup has a clear advantage over the classical Gaussian model. The main reason for this behavior has been depicted in Figure 2: To accommodate fat tails, the Gaussian setup generally produces distributions that are flatter in the center than under the NTS assumption. However, when the barriers of KO warrants are close enough to the current underlying level, this leads to a significant overestimation of knock-out risks and, hence, a lower price. Moreover, we can – maybe in some heuristic sense – interpret our findings with respect to hedging strategies. Since perfect delta-hedging is impossible due to the unremovable jump risk in the NTS setup[12], we can expect prices to be generally higher as well.

To summarize our empirical findings, in general, the NTS model performs better than the classical Black-Scholes setup, although parameter instability might be a concern. We will tackle this identification issue in the next section.

5. Compo options and a new calibration algorithm

As discussed in the previous section, by considering real market prices, the Black-Scholes as well as the NTS setup are not uniquely identified when using only quanto pricing formulas to calibrate risk neutral parameters. Mathematically, this can be seen directly for the Black-Scholes model from equation (1), as

$$\sigma_X^2 - 2\rho\sigma_X\sigma_Y + \sigma_Y^2 = A, \quad \sigma_Y^2 - \sigma_X\sigma_Y = B,$$

can have infinitely many solutions for given A and B. The same is true for the NTS assumption as it contains the Black-Scholes model. This problem is also well-known for other Lévy-based market setups and has led to stepwise calibration algorithms (see, for example, the recent study of Guillaume (2013)) or the reduction of the given parameter space by combining historical estimation and classical calibration (cf. Guillaume and Schoutens (2012) about a similar discussion for the Heston stochastic volatility model).

A common procedure for quanto options applied by practitioners is to calibrate the Gaussian model via compo options. Based on the market setup in Assumption 2.2, the implied FX volatility, σ_Y, can be identified by just using FX options. For compo equity derivatives, however, the correlation, ρ, and the implied equity volatility, σ_X, come into play leading to a similar identification issue as with just using quanto options. As, for example, pointed out by e.g. Ballotta et al. (2015), traders usually set ρ to the historical market correlation and then calibrate σ_Y and σ_X. This has

[12] See the discussion in the concluding section in Kim et al. (2015)

the additional charm that one can adjust ρ for quanto options to reflect the fact that these derivatives are typically more difficult to hedge. In fact, Ballotta et al. (2015) showed that there are significant differences between the historical and the quanto implied correlations. Therefore, for the Gaussian case we adopt the following calibration algorithm:

Algorithm BS

Step 1: Calibrate σ_Y via compo options on $1/F$.

Step 2: Take the historical correlation $\rho = 0.2216$ (based on the roughly 12-year sample in Section 2) and calibrate σ_X via compo options on N.

Step 3: Use the implied volatilities σ_X and σ_Y obtained in Step 2 and calibrate ρ via quanto options on N.

Note that this procedure can be compared to that in Brigo and Alfonsi (2005) who calibrated interest and credit rates separately as they showed that the correlation impact on theoretical CDS prices is fairly small. Our argument here is somewhat different, but leads to a comparably simple and straightforward calibration algorithm. From a theoretical perspective we need to extend the presented pricing formulas to compo options. Even though this is a straightforward calculation, we are not aware of the relevant Black-Scholes formula in the rather scarce quanto pricing literature. Therefore, in the following, we will develop and prove the pricing formula, which also leads to a better understanding of the mathematical difficulties arising for the NTS model.

5.1 Theorem. *Given Assumption 2.2 and Theorem 2.3 with $T > 0$, the prices $\mathcal{C}_t^{N,\text{compo}}(K,T)$ and $\mathcal{C}_t^{F,\text{compo}}(K,T)$ of European compo call options on $N(T)$ and $1/F(T)$ with strike $K > 0$ at time $0 \le t < T$ can be calculated via*

$$\begin{aligned}
&\mathcal{C}_t^{N,\text{compo}}(K,T) = \exp\{-r_d(T-t)\}\mathbb{E}^{\mathbb{Q}}[F(T)(N(T)-K)^+|\mathcal{F}_t] \\
&= \begin{cases} \frac{1}{\sqrt{2\pi}}\int_{\mathbb{R}}\left[V(t)\Phi(d_1[\eta]) - KF(t)e^{-r_f(T-t)}\Phi(d_2[\eta])\right]e^{-\frac{1}{2}\eta^2}d\eta & \sigma_Y\rho \neq \sigma_X \\ V(t)\Phi(d_1^0) - KF(t)e^{-r_f(T-t)}\Phi(d_2^0) & \sigma_Y\rho = \sigma_X \end{cases}
\end{aligned} \tag{5}$$

where

$$\begin{aligned}
d_1[\eta] &= \frac{\log\left(\frac{V(t)}{KF(t)}\right) + (r_f + \frac{1}{2}[\sigma_X^2 + \sigma_Y^2 - 2\sigma_X\sigma_Y\rho])(T-t)}{|\sigma_Y\rho - \sigma_X|\sqrt{T-t}} - \frac{\sqrt{1-\rho^2}}{|\rho - \sigma_X/\sigma_Y|}\eta, \\
d_2[\eta] &= d_1[\eta] - \left(|\sigma_Y\rho - \sigma_X| + \frac{\sigma_Y(1-\rho^2)}{|\rho - \sigma_X/\sigma_Y|}\right)\sqrt{T-t}
\end{aligned}$$

and

$$d_1^0 = \frac{\log\left(\frac{V(t)}{KF(t)}\right) + (r_f - \frac{1}{2}[\sigma_X^2 - \sigma_Y^2])(T-t)}{\sigma_Y\sqrt{1-\rho^2}\sqrt{T-t}}, \quad d_2^0 = d_1^0 - \sigma_Y\sqrt{1-\rho^2}\sqrt{T-t}.$$

Furthermore, we have

$$\begin{aligned}
&\mathcal{C}_t^{F,\text{compo}}(K,T) = \exp\{-r_d(T-t)\}\mathbb{E}^{\mathbb{Q}}\left[\left(\frac{\frac{1}{F(T)} - K}{\frac{1}{F(T)}}\right)^+\middle|\mathcal{F}_t\right] \\
&= \Phi(-d_2)e^{-r_d(T-t)} - e^{-r_f(T-t)}\Phi(-d_1)KF(t)
\end{aligned} \tag{6}$$

where

$$d_1 = \frac{\log(KF(t)) + \left(r_d - r_f + \frac{\sigma_Y^2}{2}\right)(T-t)}{\sigma_Y\sqrt{T-t}}, \quad d_2 = d_1 - \sigma_Y\sqrt{T-t}.$$

Proof. We start with the quanto equity option. Assume $\sigma_Y\rho > \sigma_X$ and decompose via

$$\begin{aligned}
& \mathcal{C}_t^{N,\text{compo}}(K,T) = \exp\{-r_d(T-t)\}\mathbb{E}^{\mathbb{Q}}[F(T)(N(T)-K)^+|\mathcal{F}_t] \\
= \;& \exp\{-r_d(T-t)\}\mathbb{E}^{\mathbb{Q}}[(V(T)-KF(T))^+|\mathcal{F}_t] \\
= \;& \exp\{-r_d(T-t)\}\Big\{\underbrace{\mathbb{E}^{\mathbb{Q}}[\mathbf{1}_{\{V(T)\geq KF(T)\}}V(T)|\mathcal{F}_t]}_{:=(I)} - K\underbrace{\mathbb{E}^{\mathbb{Q}}[\mathbf{1}_{\{V(T)\geq KF(T)\}}F(T)|\mathcal{F}_t]}_{:=(II)}\Big\}
\end{aligned}$$

Now set

$$d_1^\star = \frac{\log\left(\frac{V(t)}{KF(t)}\right) + (r_f - \frac{1}{2}[\sigma_X^2 - \sigma_Y^2])(T-t) - \sigma_Y\sqrt{1-\rho^2}][\bar{B}_Y(T) - \bar{B}_Y(t)]}{(\sigma_Y\rho - \sigma_X)\sqrt{T-t}}$$

then the first term becomes

$$\begin{aligned}
(I) \;=\; & V(t)\mathbb{E}^{\mathbb{Q}}\Big[\mathbb{E}^{\mathbb{Q}}\Big[\mathbf{1}_{\{V(T)\geq KF(T)\}}\frac{V(T)}{V(t)}\Big|\mathcal{F}_t \vee \mathcal{F}_\infty^{\bar{B}_Y}\Big]\Big|\mathcal{F}_t\Big] \\
= \;& V(t)\mathbb{E}^{\mathbb{Q}}\Big[(2\pi)^{-1/2}\int_{-\infty}^{d_1^\star} e^{r_d(T-t)-\frac{\sigma_X^2}{2}(T-t)+\sigma_X\sqrt{T-t}\xi}e^{-\frac{1}{2}\xi^2}d\xi\Big|\mathcal{F}_t\Big] \\
= \;& V(t)e^{r_d(T-t)}\mathbb{E}^{\mathbb{Q}}\Big[(2\pi)^{-1/2}\int_{-\infty}^{d_1^\star} e^{-\frac{1}{2}[\xi-\sigma_X\sqrt{T-t}]^2}d\xi\Big|\mathcal{F}_t\Big] \\
= \;& V(t)e^{r_d(T-t)}\mathbb{E}^{\mathbb{Q}}\Big[(2\pi)^{-1/2}\int_{-\infty}^{d_1^\star-\sigma_X\sqrt{T-t}} e^{-\frac{1}{2}\eta^2}d\eta\Big|\mathcal{F}_t\Big] \\
= \;& V(t)e^{r_d(T-t)}\mathbb{E}^{\mathbb{Q}}\Big[\Phi(d_1^\star-\sigma_X\sqrt{T-t})\Big|\mathcal{F}_t\Big] = V(t)e^{r_d(T-t)}(2\pi)^{-1/2}\int_{\mathbb{R}}\Phi(d_1[\eta])e^{-\frac{1}{2}\eta^2}d\eta
\end{aligned}$$

with $d_1[\eta]$ as in the assertion. By similar arguments, the second term can be simplified to

$$\begin{aligned}
(II) \;=\; & F(t)\mathbb{E}^{\mathbb{Q}}\Big[\mathbb{E}^{\mathbb{Q}}\Big[\mathbf{1}_{\{V(T)\geq KF(T)\}}\frac{F(T)}{F(t)}\Big|\mathcal{F}_t \vee \mathcal{F}_\infty^{\bar{B}_Y}\Big]\Big|\mathcal{F}_t\Big] \\
= \;& F(t)e^{\left(r_d-r_f+\frac{\sigma_Y^2}{2}(\rho^2-1)\right)(T-t)}\mathbb{E}^{\mathbb{Q}}\Big[e^{\sigma_y\sqrt{1-\rho^2}[\bar{B}_Y(T)-\bar{B}_Y(t)]}\Phi(d_1^\star-\sigma_Y\rho\sqrt{T-t})\Big|\mathcal{F}_t\Big] \\
= \;& F(t)e^{\left(r_d-r_f+\frac{\sigma_Y^2}{2}(\rho^2-1)\right)(T-t)}\frac{1}{\sqrt{2\pi}}\int_{\mathbb{R}} e^{\sigma_y\sqrt{(1-\rho^2)(T-t)}\eta}\Phi(d_1[\eta]-(\sigma_Y\rho-\sigma_X)\sqrt{T-t}))e^{-\frac{1}{2}\eta^2}d\eta \\
= \;& F(t)e^{(r_d-r_f)(T-t)}\frac{1}{\sqrt{2\pi}}\int_{\mathbb{R}}\Phi(d_2[\xi])e^{-\frac{1}{2}\xi^2}d\xi
\end{aligned}$$

with $d_2[\xi]$ as specified by the theorem. Combining (I) and (II), we obtain the stated formula. The cases $\sigma_Y\rho < \sigma_X$ and $\sigma_Y\rho = \sigma_X$ can be derived via similar calculations. It remains to show the formula for the compo FX option. With d_1 and d_2 as stated in the theorem, this will be done by rewriting the compo call option as K quanto put options via

$$\begin{aligned}
& \mathcal{C}_t^{F,\text{compo}}(K,T) = e^{-r_d(T-t)}\mathbb{E}^{\mathbb{Q}}\left[\left(\frac{\frac{1}{F(T)}-K}{\frac{1}{F(T)}}\right)^+\Bigg|\mathcal{F}_t\right] \\
= \;& e^{-r_d(T-t)}K\mathbb{E}^{\mathbb{Q}}[(K^{-1}-F(T))^+|\mathcal{F}_t] = e^{-r_f(T-t)-(r_d-r_f)(T-t)}K\mathbb{E}^{\mathbb{Q}}[(K^{-1}-F(T))^+|\mathcal{F}_t] \\
= \;& \Phi(-d_2)e^{-r_d(T-t)} - e^{-r_f(T-t)}\Phi(-d_1)KF(t).
\end{aligned}$$

□

Currently, we just derived prices for compo FX calls while our data set described in Section 3 includes puts of that

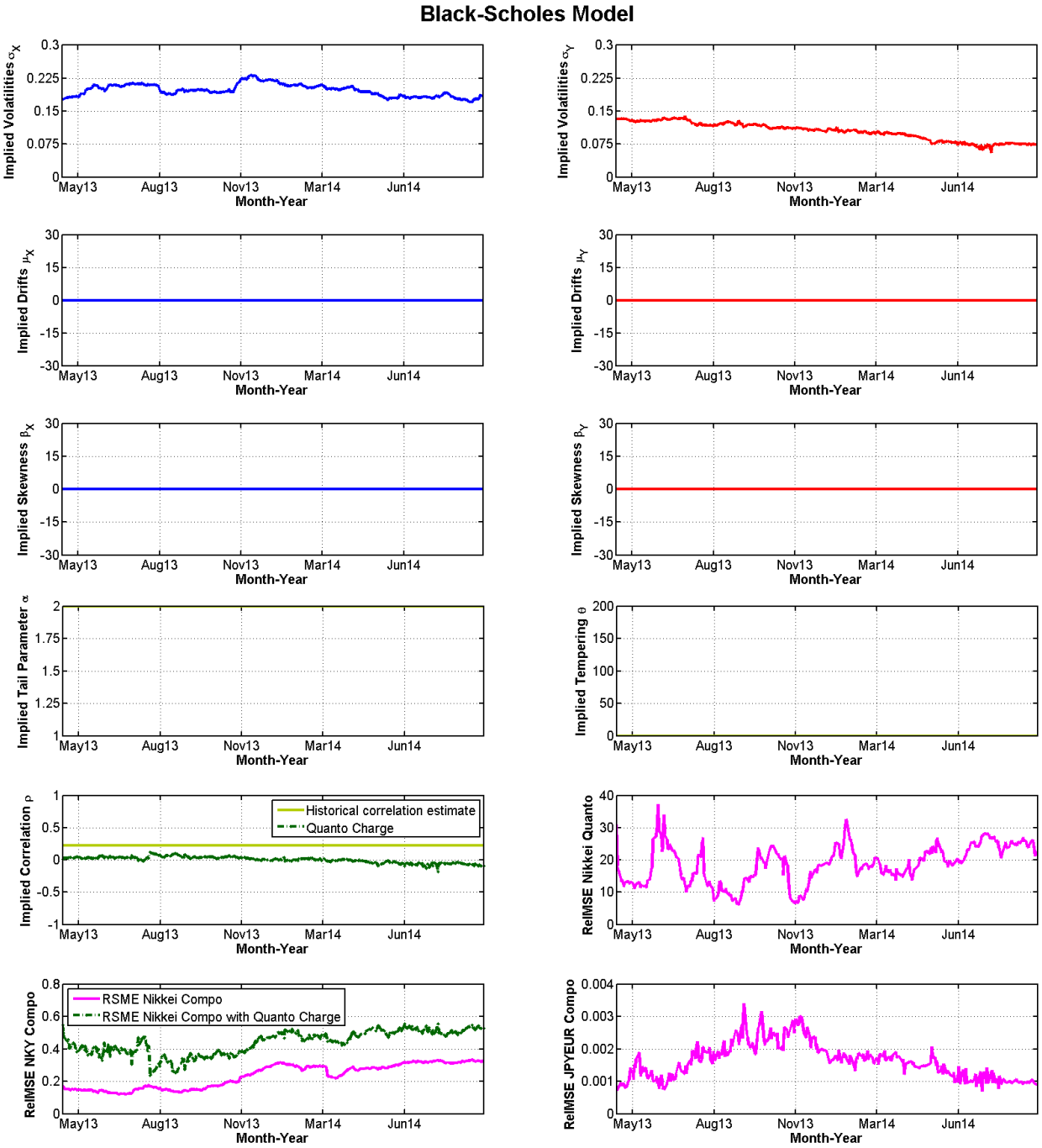

Figure 8: Quanto and compo options: daily calibrated Black-Scholes parameters and RelMSEs. All ranging from 16 April 2013 to 15 September 2014.

type as well. However, by invoking the model-free compo FX call-put-parity

$$\mathcal{P}_t^{F,\text{compo}}(K,T) = \exp\{-r_f(T-t)\}KF(t) - \exp\{-r_d(T-t)\} + \mathcal{C}_t^{F,\text{compo}}(K,T)$$

we can directly obtain the necessary put prices as well.

Figure 8 summarizes the Black-Scholes parameters obtained by the stepwise calibration algorithm. Note the following: For the equity compo options, the historical correlation of 0.2216 is used. As discussed already in Section 2, this positive correlation implies a negative correlation between the Nikkei 225 in JPY and the JPYEUR exchange rate. In Step 3 of the above calibration algorithm, the correlation is adjusted on each day to optimize the fit for Nikkei 225 quanto options. Keeping in mind that we need (4) to interpret this quanto implied correlation, we realize that even though ρ seems to be lower in absolute terms, on most days the implied relationship between the Nikkei 225 in JPY and the JPYEUR rate is even more negative, i.e., stronger.

Also, having calibrated ρ in Step 3, we examine how this correlation value affects the fit of the compo options. The RelMSEs are compared in the bottom left graph in Figure 8. It turns out that the optimal parameters for quanto substantially differ from those for the compo options. This shows that the Black-Scholes model is not able to adequately capture the increased risk contained in quanto derivatives. Therefore, one could argue that the fitted ρ values reflect a charge for this additional risk and, thus, we will refer to quanto-adjusted parameters as *quanto charge*.

For the NTS model the situation is somewhat more delicate as, especially, the tail and tempering parameters α and θ affect both option types. In addition, as shown in Section 4, the implied values of these two parameter proved to be quite instable over time. A potential solution to this problem is given in Theorem 2.5. The chosen risk-neutral measure is obtained by just modifying the drift of the two-dimensional Brownian motion and leaving the tempered stable subordinator untouched. In other words, α and θ do not change under the measure change from $\mathbb{P}$ to $\mathbb{Q}$.

As we are mainly interested in obtaining stable NTS parameters for quanto option pricing, we propose the following algorithm for the NTS framework:

Algorithm NTS

Step 1: Estimate α and θ using the bivariate log return history of V and F from Section 2.

Step 2: Calibrate the Y-parameters via compo options on $1/F$.

Step 3: Calibrate the X-parameters and the correlation ρ via compo options on N.

Step 4: Calibrate the quanto option formula by using the implied Y-parameters obtained in Step 2 but letting the X-parameters and the correlation ρ vary under the restriction that the NKY compo fit is percentage-wise not worse than the the Black-Scholes model (cf. Algorithm BS).

Note that it would also be possible to pool all options together and minimize their common RelMSE. However, that would prefer the fit for derivatives with higher prices (like the quanto options in our data set) and nearly ignore derivatives with very low prices (in our case the compo FX options).

To apply the algorithm, we need to establish the relevant compo formulas in the NTS model. At the start of the calibration procedure, α and θ are already fixed. Computationally, it helps to separate these two parameters from the others in order to increase the speed of the calibration.

5.2 Theorem. *Given Assumption 2.4 and Theorem 2.5 with $T > 0$, then the prices $\mathcal{C}_t^{N,\text{compo}}(K,T)$ and $\mathcal{C}_t^{F,\text{compo}}(K,T)$ of European compo call options on $N(T)$ and $F(T)$ with strike $K > 0$ at time $0 \le t < T$ can be calculated via*

$$\begin{aligned}\mathcal{C}_t^{N,\text{compo}}(K,T) &= \exp\{-r_d(T-t)\}\mathbb{E}^{\mathbb{Q}}[F(T)(N(T)-K)^+|\mathcal{F}_t] \\ &= \frac{1}{\sqrt{2\pi}}\int_{\mathbb{R}^+}[\mathcal{A}_{T-t}(\zeta) - K\mathcal{B}_{T-t}(\zeta)]f_{\mathcal{T}(T-t)}(\zeta)d\zeta\end{aligned}$$

where, for $\zeta > 0$,

$$f_{\mathcal{T}(T-t)}(\zeta) = \frac{1}{2\pi}\int_{\mathbb{R}} e^{-iu\zeta}\exp\Big\{-\frac{2[T-t]\theta^{1-\frac{\alpha}{2}}}{\alpha}\Big[(\theta-iu)^{\frac{\alpha}{2}} - \theta^{\frac{\alpha}{2}}\Big]\Big\}du$$

and

$$\begin{aligned}\mathcal{A}_{T-t}(\zeta) &= V(t)e^{[-w_X(\lambda_X^\star)-\beta_X](T-t)} \\ &\quad\times\int_{\mathbb{R}}\exp\left\{[\beta_X+\lambda_X^\star+\frac{\sigma_X^2}{2}(1-\rho^2)]\zeta+\rho\sigma_X\sqrt{\zeta}\eta\right\}\Phi(d_1[\eta,\zeta])e^{-\frac{1}{2}\eta^2}d\eta,\\ \mathcal{B}_{T-t}(\zeta) &= F(t)e^{(-r_f-w_Y(\lambda_Y^\star)-\beta_Y)(T-t)} \\ &\quad\times\int_{\mathbb{R}}\exp\left\{[\beta_Y+\lambda_Y^\star]\zeta+\sigma_Y\sqrt{\zeta}\eta\right\}\Phi(d_2[\eta,\zeta])e^{-\frac{1}{2}\eta^2}d\eta\end{aligned}$$

with

$$\begin{aligned}d_1[\eta,\zeta] &= d_2[\eta,\zeta]+\sigma_X\sqrt{1-\rho^2}\sqrt{\zeta}\\ d_2[\eta,\zeta] &= \frac{\log\left(\frac{V(t)}{KF(t)}\right)+[r_f+w_Y(\lambda_Y^\star)-w_X(\lambda_X^\star)+\beta_Y-\beta_X](T-t)+(\beta_X+\lambda_X^\star-\beta_Y-\lambda_Y^\star)\zeta}{\sigma_X\sqrt{1-\rho^2}\sqrt{\zeta}}\\ &\quad-\frac{(\sigma_Y-\rho\sigma_X)}{\sigma_X\sqrt{1-\rho^2}}\eta\end{aligned}$$

For the compo FX call we have

$$\begin{aligned}\mathcal{C}_t^{F,\text{compo}}(K,T) &= \exp\{-r_d(T-t)\}\mathbb{E}^{\mathbb{Q}}\left[\left(\frac{\frac{1}{F(T)}-K}{\frac{1}{F(T)}}\right)^+\middle|\mathcal{F}_t\right]\\ &= \int_{\mathbb{R}^+}[e^{-r_d(T-t)}\Phi(-d_2[\zeta])-K\mathcal{D}_{T-t}(\zeta)]f_{\mathcal{T}(T-t)}(\zeta)d\zeta \qquad (7)\end{aligned}$$

with

$$\mathcal{D}_{T-t}(\zeta)=F(t)e^{(-r_f-w_Y(\lambda_Y^\star)-\beta_Y)(T-t)}\exp\left\{[\beta_Y+\lambda_Y^\star+\frac{\sigma_Y^2}{2}]\zeta\right\}\Phi(-d_1[\zeta])$$

where

$$\begin{aligned}d_1[\zeta] &= \frac{\log(KF(t))+\left(r_d-r_f-w_Y(\lambda_Y^\star)-\beta_Y\right)(T-t)+(\beta_Y+\lambda_Y^\star+\sigma_Y^2)\zeta}{\sigma_Y\sqrt{\zeta}},\\ d_2[\zeta] &= d_1[\zeta]-\sigma_Y\sqrt{\zeta}.\end{aligned}$$

Proof. Again we start with the compo equity option. With $\mathcal{T}$ being independent of (B_X,B_Y) we can condition on the subordinator and proceed as in the proof of Theorem 5.1:

$$\begin{aligned}&\mathcal{C}_t^{N,\text{compo}}(K,T)=\exp\{-r_d(T-t)\}\mathbb{E}^{\mathbb{Q}}[F(T)(N(T)-K)^+|\mathcal{F}_t]\\ =\;&\exp\{-r_d(T-t)\}\mathbb{E}^{\mathbb{Q}}[\mathbb{E}^{\mathbb{Q}}[(V(T)-KF(T))^+|\mathcal{F}_t\vee\mathcal{F}_\infty^{\mathcal{T}}]|\mathcal{F}_t]\\ =\;&\exp\{-r_d(T-t)\}\mathbb{E}^{\mathbb{Q}}\Big[\underbrace{\mathbb{E}^{\mathbb{Q}}[\mathbf{1}_{\{V(T)\geq KF(T)\}}V(T)|\mathcal{F}_t\vee\mathcal{F}_\infty^{\mathcal{T}}]}_{:=(I)}-K\underbrace{\mathbb{E}^{\mathbb{Q}}[\mathbf{1}_{\{V(T)\geq KF(T)\}}F(T)|\mathcal{F}_t\vee\mathcal{F}_\infty^{\mathcal{T}}]}_{:=(II)}\Big|\mathcal{F}_t\Big].\end{aligned}$$

In contrast to the Black-Scholes-type model, (B_X,B_Y) is correlated without assuming partly equal sample paths. However, using the well-known fact that conditional Gaussian random variables are again normally distributed we

obtain for $0 \le t < T$

$$\begin{aligned} & B_X(\mathcal{T}(T)) - B_X(\mathcal{T}(t)) \Big| B_Y(\mathcal{T}(T)) - B_Y(\mathcal{T}(t)), \mathcal{F}_\infty^{\mathcal{T}} \\ \sim \quad & N\Big(\rho[B_Y(\mathcal{T}(T)) - B_Y(\mathcal{T}(t))], [\mathcal{T}(T) - \mathcal{T}(t)](1-\rho^2)\Big). \end{aligned}$$

Since $\mathcal{T}(T) - \mathcal{T}(t) \neq 0$ a.s. we set

$$\begin{aligned} & d_2^\star \\ = \quad & \frac{\log\left(\frac{V(t)}{KF(t)}\right) + [r_f + w_Y(\lambda_Y^\star) - w_X(\lambda_X^\star) + \beta_Y - \beta_X](T-t) + (\beta_X + \lambda_X^\star - \beta_Y - \lambda_Y^\star)[\mathcal{T}(T) - \mathcal{T}(t)]}{\sigma_X\sqrt{1-\rho^2}\sqrt{\mathcal{T}(T) - \mathcal{T}(t)}} \\ & - \frac{(\sigma_Y - \rho\sigma_X)[B_Y(\mathcal{T}(T)) - B_Y(\mathcal{T}(t))]}{\sigma_X\sqrt{1-\rho^2}\sqrt{\mathcal{T}(T) - \mathcal{T}(t)}} \end{aligned}$$

Now we can proceed with the individual terms starting with

$$\begin{aligned} (I) \quad = \quad & V(t)\mathbb{E}^{\mathbb{Q}}\Big[\mathbb{E}^{\mathbb{Q}}\Big[\mathbf{1}_{\{V(T)\ge KF(T)\}}\frac{V(T)}{V(t)}\Big|\mathcal{F}_t \vee \sigma(B_Y(\mathcal{T}(T)) - B_Y(\mathcal{T}(t))) \vee \mathcal{F}_\infty^{\mathcal{T}}\Big]\Big|\mathcal{F}_t \vee \mathcal{F}_\infty^{\mathcal{T}}\Big] \\ = \quad & V(t)\mathbb{E}^{\mathbb{Q}}\Big[\frac{1}{\sqrt{2\pi}} \\ & \times \int_{-d_2^\star}^{\infty} \exp\Big\{[r_d - w_X(\lambda_X^\star) - \beta_X](T-t) + (\beta_X + \lambda_X^\star)[\mathcal{T}(T) - \mathcal{T}(t)]\Big\} \\ & \times \exp\Big\{\rho\sigma_X[B_Y(\mathcal{T}(T)) - B_Y(\mathcal{T}(t))] + \sigma_X\sqrt{\mathcal{T}(T) - \mathcal{T}(t)}\sqrt{1-\rho^2}\xi\Big\}e^{-\frac{1}{2}\xi^2}d\xi\Big|\mathcal{F}_t \vee \mathcal{F}_\infty^{\mathcal{T}}\Big] \\ = \quad & V(t)e^{[r_d - w_X(\lambda_X^\star) - \beta_X](T-t)} \\ & \times\mathbb{E}^{\mathbb{Q}}\Big[\exp\Big\{[\beta_X + \lambda_X^\star + \frac{\sigma_X^2}{2}(1-\rho^2)][\mathcal{T}(T) - \mathcal{T}(t)] + \rho\sigma_X[B_Y(\mathcal{T}(T)) - B_Y(\mathcal{T}(t))]\Big\} \\ & \times\frac{1}{\sqrt{2\pi}}\int_{-d_2^\star}^{\infty}\exp\Big\{-\frac{1}{2}[\xi - \sigma_X\sqrt{\mathcal{T}(T) - \mathcal{T}(t)}\sqrt{1-\rho^2}]^2\Big\}d\xi\Big|\mathcal{F}_t \vee \mathcal{F}_\infty^{\mathcal{T}}\Big] \\ = \quad & V(t)e^{[r_d - w_X(\lambda_X^\star) - \beta_X](T-t)} \\ & \times\mathbb{E}^{\mathbb{Q}}\Big[\exp\Big\{[\beta_X + \lambda_X^\star + \frac{\sigma_X^2}{2}(1-\rho^2)][\mathcal{T}(T) - \mathcal{T}(t)] + \rho\sigma_X[B_Y(\mathcal{T}(T)) - B_Y(\mathcal{T}(t))]\Big\} \\ & \times\Phi(d_2^\star + \sigma_X\sqrt{\mathcal{T}(T) - \mathcal{T}(t)}\sqrt{1-\rho^2})\Big|\mathcal{F}_t \vee \mathcal{F}_\infty^{\mathcal{T}}\Big] \\ = \quad & \frac{1}{\sqrt{2\pi}}V(t)e^{[r_d - w_X(\lambda_X^\star) - \beta_X](T-t)} \\ & \times\int_{\mathbb{R}}\exp\Big\{[\beta_X + \lambda_X^\star + \frac{\sigma_X^2}{2}(1-\rho^2)][\mathcal{T}(T) - \mathcal{T}(t)] + \rho\sigma_X\sqrt{\mathcal{T}(T) - \mathcal{T}(t)}\eta\Big\} \\ & \times\Phi(d_2^\star + \sigma_X\sqrt{\mathcal{T}(T) - \mathcal{T}(t)}\sqrt{1-\rho^2})e^{-\frac{1}{2}\eta^2}d\eta \end{aligned}$$

Moreover we have

$$\begin{aligned}
(II) &= F(t)\mathbb{E}^{\mathbb{Q}}\Big[\mathbb{E}^{\mathbb{Q}}\Big[\mathbf{1}_{\{V(T)\geq KF(T)\}}\frac{F(T)}{F(t)}\Big|\mathcal{F}_t\vee\sigma(B_Y(\mathcal{T}(T))-B_Y(\mathcal{T}(t)))\vee\mathcal{F}_\infty^{\mathcal{T}}\Big]\Big|\mathcal{F}_t\vee\mathcal{F}_\infty^{\mathcal{T}}\Big]\\
&= F(t)e^{(r_d-r_f-w_Y(\lambda_Y^\star)-\beta_Y)(T-t)}\\
&\quad\times\mathbb{E}^{\mathbb{Q}}\Big[\exp\Big\{(\beta_Y+\lambda_Y^\star)[\mathcal{T}(T)-\mathcal{T}(t)]+\sigma_Y[B_Y(\mathcal{T}(T))-B_Y(\mathcal{T}(t))]\Big\}\Phi(d_2^\star)\Big|\mathcal{F}_t\vee\mathcal{F}_\infty^{\mathcal{T}}\Big]\\
&= \frac{1}{\sqrt{2\pi}}F(t)e^{(r_d-r_f-w_Y(\lambda_Y^\star)-\beta_Y)(T-t)}\\
&\quad\times\int_{\mathbb{R}}\exp\Big\{(\beta_Y+\lambda_Y^\star)[\mathcal{T}(T)-\mathcal{T}(t)]+\sigma_Y\sqrt{\mathcal{T}(T)-\mathcal{T}(t)}\eta\Big\}\Phi(d_2^\star)e^{-\frac{1}{2}\eta^2}d\eta
\end{aligned}$$

Combining everything we obtain the assertion. The formula for the compo FX call can be derived via similar, but rather tedious, calculations. □

The following new representation for the pricing formula in Theorem 2.5 also helps to speed up Step 4 of the new calibration algorithm: As we do not need to minimize over α and θ, we can calculate upfront the subordinator density on a chosen grid and, thus, improve significantly on the otherwise supreme Fast Fourier Transform Algorithm.

5.3 Theorem. *Given Assumption 2.4 and Theorem 2.5 with $T>0$, assume $\sigma_X^2+\sigma_Y^2-2\rho\sigma_X\sigma_Y>0$. Then, for $K>0$, $F_{fix}>0$ and $0\leq t<T$, we have*

$$\begin{aligned}
C_t^{quanto}(K,T) &= \exp\{-r_d(T-t)\}\mathbb{E}^{\mathbb{Q}}[F_{fix}(N(T)-K)^+|\mathcal{F}_t]\\
&= \int_{\mathbb{R}^+}[\mathcal{E}_{T-t}(\zeta)-Ke^{-r_d(T-t)}\Phi(d_2[\zeta])]f_{\mathcal{T}(T-t)}(\zeta)d\zeta
\end{aligned}$$

where for $\zeta>0$

$$\begin{aligned}
f_{\mathcal{T}(T-t)}(\zeta) &= (2\pi)^{-1}\int_{\mathbb{R}}e^{-iu\zeta}\exp\Big\{-\frac{2[T-t]\theta^{1-\frac{\alpha}{2}}}{\alpha}\Big[(\theta-iu)^{\frac{\alpha}{2}}-\theta^{\frac{\alpha}{2}}\Big]\Big\}du,\\
\mathcal{E}_{T-t}(\zeta) &= N(t)e^{[-r_d+r_f+w_Y(\lambda_Y^\star)+\beta_Y-w_X(\lambda_X^\star)-\beta_X](T-t)}\\
&\quad\times\exp\Big\{[\beta_X+\lambda_X^\star-\beta_Y-\lambda_Y^\star+\frac{1}{2}(\sigma_X^2+\sigma_Y^2-2\rho\sigma_X\sigma_Y)]\zeta\Big\}\Phi(d_1[\zeta])
\end{aligned}$$

with

$$\begin{aligned}
d_1[\zeta] &= d_2[\zeta]+\sqrt{\sigma_X^2+\sigma_Y^2-2\rho\sigma_X\sigma_Y}\sqrt{\zeta},\\
d_2[\zeta] &= \frac{\log\left(\frac{N(t)}{K}\right)+\Big(r_f+w_Y(\lambda_Y^\star)-w_X(\lambda_X^\star)+\beta_Y-\beta_X\Big)(T-t)+(\beta_X+\lambda_X^\star-\beta_Y-\lambda_Y^\star)\zeta}{\sqrt{\sigma_X^2+\sigma_Y^2-2\rho\sigma_X\sigma_Y}\sqrt{\zeta}}
\end{aligned}$$

Proof. The proof follows along the lines of Theorem 5.2 and involves, again, a tedious calculation. □

The results obtained for the NTS model are illustrated in Figure 9. One of our main findings is that when fixing α and θ upfront and including compo options, the calibrated parameters (especially drift and skewness) are much more stable over time than when just considering quanto options as done in Section 4. Even though some quanto implied parameters (i.e., quanto charges) are quite different than those coming from the Nikkei compo options, the two RelMSEs (bottom left) do not differ as much as in the Black-Scholes setting. This is inline with our earlier findings on the KO option fit in Section 4: The NTS model generally seems to be coping much better with the additional quanto risk. This is especially obvious between November 2013 and March 2014.

Finally, as in Section 4, we use the calibrated parameters to calculated *delta-based* forecasts for the quanto options and compare the out-of-sample model fit for our double-barrier option data. The daily RelMSE differences (including those for the calibration fit) are shown in Figure 10.

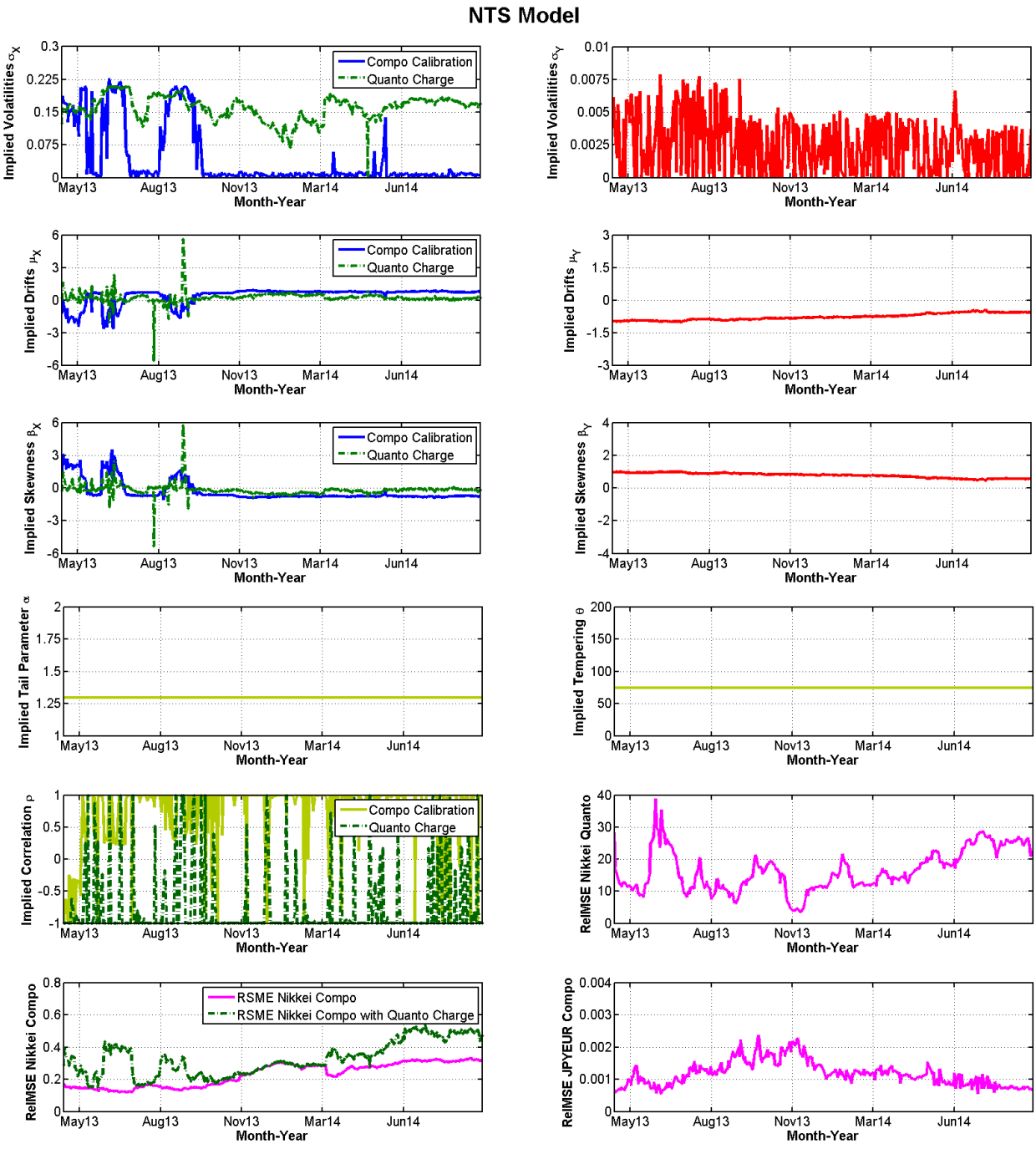

Figure 9: Quanto and compo options: daily calibrated (X,Y) NTS parameters and RelMSEs. All ranging from 16 April 2013 to 15 September 2014.

When having α and θ fixed at the chosen values, our two models do now clearly differ and therefore it is nor surprising that on some days, the quanto fit for the Black-Scholes setup might be better. This can be seen especially for the last months of our chosen time frame where Figure 6 implied α-values close to 2. However, when considering the complete observation period, the NTS setup is still clearly supreme to the Gaussian model for quanto and also especially for FX compo options. Interestingly, even though the Nikkei compo fit is nearly the same (second row of Figure 10), the additional quanto charge is lower for the NTS model.

Also when looking at the *delta-based* forecasts for quanto options, the NTS setup implies more stable parameters over time than the Black-Scholes model.

Finally, for the double-barrier options, the NTS framework clearly outperforms the Black-Scholes setup again even though its advantage is lower than in Section 4. However this can be explained by the fact that the additional compo options make it harder for every model.

Summary

We carried out a throughout empirical study on quanto retail options comparing a classical Black-Scholes type market and the newly proposed NTS framework of Kim et al. (2015) over a period of 17 months on a daily basis. Our results show that the latter (which is contained in the general Lévy class) does not only perform better when calibrated to quoted prices of classical quanto call options but also shows a better forecasting ability measured in terms of a *delta-based* forecast. The arising issues of identification and parameter stability are tackled by stepwise calibration procedures using compo options. Additionally, when comparing the out-of-sample fit by pricing exotic double-barrier options, the Gaussian setup is clearly outperformed, as well.

Baeumer, B., Meerschaert, M. M., 2010. Tempered stable Lévy motion and transit super-diffusion. Journal of Computational and Applied Mathematics 233 (10), 2438–2448.

Ballotta, L., Deelstra, G., G., R., 2015. Quanto implied correlation in a Multi-Lévy framework, available online at: http://papers.ssrn.com/sol3/papers.cfm?abstract_id=2569015.

Barndorff-Nielsen, O. E., Levendorskii, S., 2001. Feller processes of normal inverse Gaussian type. Quantitative Finance 1, 318–331.

Barndorff-Nielsen, O. E., Shephard, N., 2001. Normal modified stable processes. Department of Economics, Discussion Paper Series, University of Oxford 72.

Baxter, M., Rennie, A., 1996. Calculus: An Introduction to Derivative Pricing. Cambridge University Press.

Bianchi, M. L., Rachev, S. R., Kim, Y. S., Fabozzi, F. J., 2010. Tempered stable distributions and processes in finance: numerical analysis. In: Corazza, M., Pizzi, C. (Eds.), Mathematical and Statistical Methods for Actuarial Sciences and Finance. Springer.

Branger, N., Muck, M., 2012. Keep on smiling? The pricing of Quanto options when all covariances are stochastic. Journal of Banking & Finance 36, 1577–1591.

Brigo, D., Alfonsi, A., 2005. Credit default swap calibration and derivatives pricing with the SSRD stochastic intensity model. Finance and Stochastics 9 (1), 29–42.

Broadie, M., Glasserman, P., 1997. A continuity correction for discrete barrier options. Mathematical Finance 7 (4), 325–348.

Carr, P., Madan, D., 1999. Option pricing and the Fast Fourier Transform. Journal of Computational Finance 2 (4), 61—-73.

Chen, A. H., Kensinger, J. W., 1990. An analysis of market-index certificates of deposit. Journal of Financial Services Research 4, 93–110.

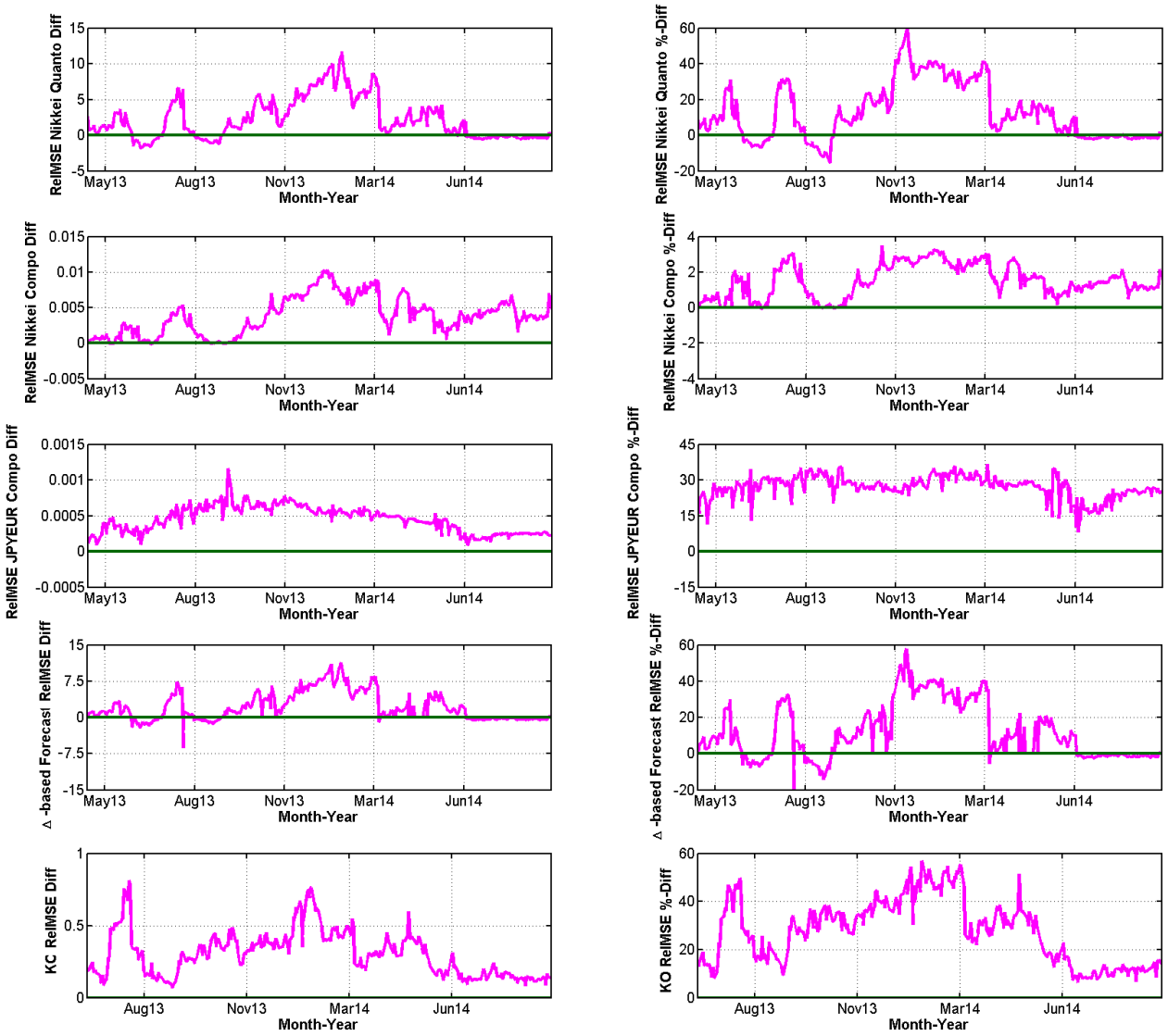

Figure 10: Quanto, compo and KO options. Top three: RelMSE-difference for the quanto Nikkei, compo Nikkei and JPYEUR options. Bottom two: RelMSE-difference of the *delta-based* forecasts of quanto Nikkei call prices and RelMSE-difference for KO options. Vanilla options ranging from 16 April 2013 to 15 September 2014, KO options from 19 June 2013 to 15 September 2014. Positive values indicate better performance of the NTS model.

Chen, K. C., Sears, R. S., 1990. Pricing the SPIN. Financial Management 19, 36–47.

Delbaen, F., Schachermayer, W., 1994. A general version of the fundamental theorem of asset pricing. Math. Annalen 312, 463–520.

Derman, E., Karasinski, P., Wecker, J. S., 1990. Understanding guaranteed exchange-rate contracts in foreign stock investments. Goldman Sachs Quantitative Strategies Research Notes.

Dimitroff, G., Szimayer, A., Wagner, A., 2009. Quanto option pricing in the parsimonious Heston model. Berichte des Fraunhofer ITWM 174.

Eberlein, E., Glau, K., 2014. Variational solutions of the pricing PIDEs for European options in Lévy models. Applied Mathematical Finance 21, 417–450.

Eberlein, E., Glau, K., Papapantoleon, A., 2009. Analyticity of the Wiener-Hopf factors and valuation of exotic options in Lévy models. Advanced Mathematical Methods for Finance, 223–245.

Eberlein, E., Glau, K., Papapantoleon, A., 2010. Analysis of Fourier transform valuation formulas and applications. Applied Mathematical Finance, 211–240.

Eberlein, E., Keller, U., 1995. Hyperbolic distributions in finance. Bernoulli 1, 281–299.

Eberlein, E., Keller, U., Prause, K., 1998. New insights into smile, mispricing and value at risk: the hyperbolic model. Journal of Business 71, 371–405.

Escobar, M., P., H., Scherer, M., 2014. Efficiently pricing double barrier derivatives in stochastic volatility models. Review of Derivatives Research 17 (2), 191–216.

Fink, H., Geissel, S., Sass, J., Seifried, F. T., 2016. Implied risk aversion: An alternative rating system for retail structured products., available online at: http://papers.ssrn.com/sol3/papers.cfm?abstract_id=2651135.

Geman, H., Yor, M., 1996. Pricing and hedging double-barrier options: a probabilistic approach. Mathematical Finance 6, 365–378.

Guillaume, F., 2013. The αVG model for multivariate asset pricing: calibration and extension. Review of Derivatives Research 16 (1), 25–52.

Guillaume, F., Schoutens, W., 2012. Calibration risk: Illustrating the impact of calibration risk under the Heston model. Review of Derivatives Research 15 (1), 57–79.

Kawai, R., Masuda, H., 2012. Infinite variation tempered stable Ornstein-Uhlenbeck processes with discrete observations. Communications in Statistics - Simulation and Computation 41 (1), 125–139.

Kim, Y. S., Giacometti, R., Rachev, S. T., Fabozzi, F. J., Mignacca, D., 2012. Measuring financial risk and portfolio optimization with a non-Gaussian multivariate model. Annals of Operations Research 201 (1), 325–343.

Kim, Y. S., Lee, J., Mittnik, S., Park, J., 2015. Quanto option pricing in the presence of fat tails and asymmetric dependence. Journal of Econometrics 187, 512–520.

Kunitomo, N., Ikeda, M., 1992. Pricing options with curved boundaries. Mathematical Finance 2 (4), 275–298.

Park, J., Lee, Y., Lee, J., 2013. Pricing of quanto option under the Hull and White stochastic volatility model. Communications of the Korean Mathmatical Society 28 (3), 615–633.

Sato, K.-I., 1999. Lévy Processes and Infinitely Divisible Distributions. Cambridge University Press, Cambridge.

Schoutens, W., Van Damme, G., 2011. The β-variance gamma model. Review of Derivatives Research 14 (3), 263–282.

Stoimenov, P. A., Wilkens, S., 2005. Are structured products 'fairly' priced? An analysis of the german market for equity-linked instruments. Journal of Banking and Finance 29, 2971–2993.

Teng, L., Ehrhardt, M., Günther, M., 2015. The pricing of quanto options under dynamic correlation. Journal of Computational and Applied Mathematics 275, 304–310.

Wilkens, S., Erner, C., Röder, K., 2003. The pricing of structured products in germany. Journal of Derivatives 11, 55–69.

Wilmott, P., 2006. Paul Wilmott on Quantitative Finance. John Whiley & Sons, Ltd.

Appendix

The following RSPs were used in this empirical study:

Nikkei 225 open-end-tracker: 252140, 698516, 702976, 787332, CB5UYN, HV1NKY, DR1CD5, DZ2NX7, DZ2RZC

Nikkei 225 quanto call options: SG3424, SG3425, SG3426, SG3427, SG3428, SG3429, SG343A, SG343B, SG343C, SG343D, SG343E, SG343F, SG343G, SG343H, SG343J, SG343K, SG343L, SG343M, SG343N, SG343P, SG343Q, SG343R, SG343S, SG343T, SG343U, SG343V, SG343W, SG343X, SG343Y

Nikkei 225 compo call options: SG196L, SG196M, SG3WBJ, SG3WBK, SG3WBL, SG3WBM, SG3WBP, SG3WBQ, SG3WBR, SG3WBS, SG3WBT, SG3WBU, SG3WBV, SG2L0T, SG2L0U, SG2L0V, SG2L0W, SG2WQW, SG2WQX, SG2WQY

EURJPY compo options: SG3W6J, SG3W6K, SG3W6L, SG3W6M, SG3W6N, SG3W6P, SG3W6Q, SG3W6R, SG3W6S, SG3W6T, SG3W6U, SG3W6V, SG3W6W, SG3W6X, SG3W6Y, SG3W6Z, SG3W60, SG3W61

Nikkei 225 KO options: SG36ET, SG36EV, SG36EY, SG36EZ, SG36E0, SG36E1, SG36E4, SG4EFS, SG4EFT, SG4EFU, SG4EFV, SG4EFW, SG4EFX, SG4EFY, SG4EFZ, SG4EF0, SG4EF1, SG4EF2, SG4EF3, SG4EF4, SG4EF5, SG4EF6, SG4EF7, SG4EF8, SG4EF9, SG4EGA, SG4EGB, SG4EGC, SG4EGD, SG4EGE, SG4EGF, SG4EGG, SG4EGH, SG4EGJ, SG4EGK, SG4EGL, SG4EGM, SG4EGN, SG4EGP, SG4EGQ, SG4EGR, SG4EGS, SG4EGT, SG4EGU, SG4EGV, SG4EGW, SG4EGX, SG4EGY, SG4FZL, SG4FZM, SG4FZN, SG4FZP, SG4FZQ, SG4FZT, SG4FZU, SG4FZV, SG4FZW, SG4FZX, SG4FZZ, SG4FZ0, SG4FZ1, SG4FZ2, SG4FZ3, SG4FZ4, SG4FZ5, SG4FZ6, SG4FZ7, SG4FZ8, SG4FZ9, SG4F0A, SG4F0B, SG4F0C, SG4F0D, SG4F0E, SG4F0F, SG4NCZ, SG4NC0, SG4NC1, SG4NC2, SG4NC3, SG4NC4, SG4NC5, SG4NC6, SG4NC7, SG4NC8, SG4NC9, SG4NDA, SG4NDB, SG4NDC, SG4NDD, SG4S20, SG4S21, SG4S22, SG4S23, SG4S24, SG4S25, SG4S26, SG4S27, SG4S28, SG4S29, SG4S3A, SG4S3B, SG4S3C, SG4S3D, SG4S3E, SG4S3F, SG4S3G, SG4S3H, SG4S3J, SG4S3K, SG4S3L, SG4S3M, SG4S3N, SG4S3P, SG4S3Q, SG4S3R, SG4S3S, SG4S3T, SG4S3U, SG4S3V, SG4S3W, SG4S3X, SG4S3Y, SG4S3Z, SG4S30, SG41DF, SG41DG, SG41DH, SG41DJ, SG41DK, SG41DL, SG41DM, SG41DN, SG41DP, SG41DQ, SG41DR, SG41DS, SG41DT, SG42UV, SG42UW, SG42UX, SG42UY, SG42UZ, SG42U0, SG42U1, SG42U2, SG42U3, SG42U4, SG42U5, SG42U6, SG42U7, SG42U8, SG42U9, SG42VA, SG42VB, SG42VC, SG42VD, SG42VE, SG42VF, SG42VG, SG42VH, SG42VJ, SG42VK, SG42VL, SG42VM, SG42VN, SG42VP, SG4739, SG474A, SG474B, SG474C, SG474D, SG474E, SG474F, SG474G, SG474H, SG474J, SG474K, SG474L, SG474M, SG474N, SG474P, SG474Q, SG474R, SG474S, SG474T, SG474U, SG474V, SG474L, SG474X, SG474Y, SG474Z, SG4740, SG4741, SG4742, SG4743, SG4744, SG4745, SG4746, SG4747, SG4748, SG4749, SG475A, SG475B, SG475C, SG475D, SG475E, SG475F, SG475G, SG475H, SG475J, SG475K, SG475L, SG475M, SG475N, SG475P, SG475Q, SG475R, SG475S, SG475T, SG475U, SG475V, SG475W, SG475X, SG475Y, SG475Z, SG4750, SG4751, SG4752, SG4753, SG4754, SG4755, SG4756, SG5BFZ, SG5BF0, SG5BF1, SG5BF2, SG5BF3, SG5BF4, SG5BF5, SG5BF6, SG5BF7, SG5BF8, SG5BF9, SG5BGA, SG5BGB, SG5BGC, SG5BGD, SG5LUU, SG5LUV, SG5LUW, SG5LUX, SG5LUY, SG5LUZ, SG5LU0, SG5LU1, SG5LU2, SG5LU3, SG5LU4, SG5LU5, SG5LU6, SG5LU7, SG5LU8, SG5LU9, SG5LVA, SG5LVB, SG5LVC, SG5LVD, SG5LVE, SG5LVF, SG5LVG, SG5LVH, SG5LVJ, SG5LVK, SG5LVL, SG5LVM, SG5LVN, SG5LVP, SG5LVQ, SG5LVR, SG5LVS, SG5LVT, SG5LVU, SG5LVV, SG5NVU, SG5NVV, SG5NVW, SG5NVX, SG5NVY, SG5NVZ, SG5NV0, SG5NV1, SG5NV2, SG5NV3, SG5NV4, SG5NV5, SG5NV6, SG5NV7, SG5NV8, SG5NV9, SG5NWA, SG5NWB, SG5NWC, SG5NWD, SG5NWE, SG5NWF, SG5NWG, SG5NWH, SG5NWJ, SG5NWK, SG5NWL, SG5NWM, SG5QKA, SG5QKB, SG5QKC, SG5QKD, SG5QKE, SG5QKF, SG5QKG, SG5QKH, SG5QKJ, SG5QKK, SG5QKL, SG5QKM, SG5QKN, SG5QKP, SG5QKQ, SG5QKR, SG5QKS, SG5QKT, SG5QKU, SG5QKV, SG5QKW, SG5QKX, SG5QKY, SG5QKZ, SG5QK0, SG5QK1, SG5QN3, SG5QN4, SG5VQL, SG5VQM, SG5VQN, SG5VQP, SG5VQQ, SG5VQR, SG5VQS, SG5VQT, SG5VQU, SG5VQV, SG5VQW, SG5VQX, SG5VQY, SG5VQZ, SG5VQ0, SG5VQ1, SG5VQ2, SG5V0G, SG5V0H, SG5V0J, SG5V0K, SG5V0L, SG5V0M